

SHOALING OF REGULAR AND RANDOM
WAVES ON A BEACH OF CONSTANT SLOPE

A Thesis submitted
in Partial Fulfilment of the Requirements
for the Degree of
MASTER OF TECHNOLOGY

by

RAJESH MISHRA

to the

DEPARTMENT OF CIVIL ENGINEERING
INDIAN INSTITUTE OF TECHNOLOGY KANPUR
DECEMBER 1994

- 9 i... 1995/CE

1995
1995

Rec. No. A. 118764

CE-1994-M
MIS-S



A118764

CE-1994-M-~~SHO~~MIS-SHO

C E R T I F I C A T E

It is certified that the work contained in this thesis entitled "SHOALING OF REGULAR AND RANDOM WAVES ON A BEACH OF CONSTANT SLOPE", by RAJESH MISHRA, has been carried out under our supervision and this work has not been submitted elsewhere for the degree.

S. Surya Rao

Dr S. SURYA RAO

PROFESSOR

DEPTT. OF CIVIL ENGG.

I.I.T. KANPUR

K Muralidhar

Dr K. MURALIDHAR

ASSOCIATE PROFESSOR

DEPTT. OF MECH. ENGG.

I.I.T. KANPUR

DECEMBER, 1994

DEDICATION

I RESPECTFULLY DEDICATED THIS DISSERTATION

TO
MY PARENTS

FOR ALL THE LOVE, SUPPORT AND UNDERSTANDING
THEY HAVE GIVEN TO ME THROUGHOUT MY LIFE

ACKNOWLEDGEMENT

The author wishes to express his most sincere gratitude and appreciation to his thesis advisors Dr. S. Surya Rao and Dr. K. Muralidhar for their valuable guidance, inspiration and encouragement during the course of this work.

Sincere thanks are also extended to Dr. B. Dutta, Dr. K. Subramanya, Dr. S. Ramaseshan and Dr. S. S. Rao of the department of civil engineering for the thought-provoking courses he has received from them during the degree programme.

The author wishes to place on record the kind gesture and cooperation given by Shri Suresh Kumar, Shri Kalyandas, Shri Ram Shankar, Shri J. C. Gupta and Shri Sita Ram who gave him their full support during his experimental work.

The encouragement and unreserved help received from all his friends specially B. K. Jha, Rajesh Singh, B. K. Pandey, P. M. V. Subbarao, S. P. Singh and Bhim Singh during the various stages of the thesis is gratefully acknowledged.

A B S T R A C T

The mechanism of transformation in shoaling of waves is one of the fundamental problems in coastal engineering. For efficient and reliable design of coastal structures it is very important to know the shallow water wave characteristics. In the present investigation an experimental study of the transformation of waves as they propagate from deep water to shallow water is presented. Regular waves and random waves are generated in a wave flume with a sloping beach in the laboratory. Random waves generated have JONSWAP spectra. Results show that the phase velocity measured is close to that obtained by using small amplitude wave theory. Essential differences with the linear dispersion relation have been found for random waves. The spectral peak for wave height decreases with decrease in water depth. This shows increasing nonlinearity with decreasing depth but is in agreement with published literature. The frequency corresponding to the spectral peak increases with decreasing water depth.

TABLE OF CONTENTS

	PAGE
CERTIFICATE	
ACKNOWLEDGEMENT	1
ABSTRACT	i i
LIST OF FIGURES	v
LIST OF TABLES	vii
LIST OF PHOTOGRAPHS	viii
LIST OF SYMBOLS	ix
CHAPTER I INTRODUCTION	1
CHAPTER II LITERATURE REVIEW	
2.1 SHOALING OF REGULAR WAVES	4
2.2 MODELS FOR SPECTRA	7
2.3 SHOALING OF RANDOM WAVES	8
CHAPTER III EXPERIMENTAL DETAILS	
3.1 EQUIPMENT	11
3.2 SPECIFICATIONS	20
3.3 PROCEDURE	22
CHAPTER IV RESULTS AND DISCUSSION	25
CHAPTER V CONCLUSIONS	55
REFERENCES	56
APPENDIX A MEASURED SIGNALS	58

APPENDIX B	DEFINITION OF IMPORTANT PARAMETERS AND METHOD OF THEIR CALCULATION	62
APPENDIX C	LISTING OF PROGRAMMES	
	C.1 PROGRAMME FOR SCALING THE SIGNAL DATA	65
	C.2 PROGRAMME TO CALCULATE WAVENUMBER AND CELERITY FOR RANDOM WAVES	66
	C.3 PROGRAMME TO CALCULATE WAVE SPECTRUM	69
	C.4 PROGRAMME TO CALCULATE ENERGY FLUX	71
	C.5 PROGRAMME TO CALCULATE SPECTRUM WIDTH PARAMETER	72
	C.6 PROGRAMME TO GENERATE REGULAR WAVES	73
	C.7 PROGRAMME TO GENERATE RANDOM WAVES	74

LIST OF FIGURES

FIGURES	PAGE
2.1 Shoaling curves for regular waves	5
3.1 A Schematic Illustration of the wave flume	15
3.2 A Schematic Illustration of wavemaker	16
4.1 H/H_0 versus h/L_0 for regular waves	34
4.2 η/η_0 versus h/L_0 for regular waves	35
4.3 C/C_0 versus h/L_0 for regular waves	36
4.4 C_g/C versus h/L_0 for regular waves	37
4.5 P versus h/L_0 for regular waves	38
4.6 $S(\omega)$ versus ω/ω_p for different water depths (CASE 1)	39
4.7 $S(\omega)$ versus ω/ω_p for different water depths (CASE 2)	40
4.8 $S(\omega)$ versus ω/ω_p for different water depths (CASE 3)	41
4.9 $S(\omega)$ versus ω/ω_p for $h = 70$ cm	42
4.10 $S(\omega)$ versus ω/ω_p for $h = 67.5$ to 52.5 cm	43
4.11 $S(\omega)$ versus ω/ω_p for $h = 47.5$ to 32.5 cm	44
4.12 $S(\omega)$ versus ω/ω_p for $h = 27.5$ to 15.0 cm	45
4.13 Comparison of theoretical and measured dispersion relation for random waves for $h = 67.5$ to 47.5 cm	46
4.14 Comparison of theoretical and measured dispersion relation for random waves	

	for h = 42.5 to 27.5 cm	47
4.15	Comparison of theoretical and measured dispersion relation for random waves	
	for h = 22.5 to 12.5 cm	48
4.16	Comparison of theoretical and measured dispersion relation for random waves	
	for h = 7.5 to 5.0 cm	49
4.17	Measured component phase velocity normalised by its deep water value for random waves for h = 42.5 to 27.5 cm	50
4.18	Measured component phase velocity normalised by its deep water value for random waves for h = 67.5 to 47.5 cm	51
4.19	Measured component phase velocity normalised by its deep water value for random waves for h = 70.0	52
4.20	$\bar{\omega}/\omega_0$ versus $K_p h$ (Experimental results)	53
4.21	$\omega_p/\bar{\omega}$ versus $K_p h$	54
A.1	Water surface records for regular waves	58
A.2	Water surface records for random waves (CASE 1)	59
A.3	Water surface records for random waves (CASE 2)	60
A.4	Water surface records for random waves (CASE 3)	61

LIST OF TABLES

	PAGE
TABLE 3.1 Parameters of JONSWAP spectra	24
TABLE 4.1 Calculation of wave height and r. m. s. wave height for regular waves	29
TABLE 4.2 Calculation of C/C_0 , C/C_g , P_1 and P_2 for regular waves	30
TABLE 4.3 Calculatin of coherence factor, spectrum width parameter and energy flux for random waves (CASE 1)	31
TABLE 4.4 Calculatin of coherence factor, spectrum width parameter and energy flux for random waves (CASE 1)	32
TABLE 4.5 Calculatin of coherence factor, spectrum width parameter and energy flux for random waves (CASE 1)	33

LIST OF PHOTOGRAPHS

	PAGE
Photo. 1 Photograph showing the wave flume with piping for filling and emptying the wave flume and wave monitor	17
Photo. 2 Photograph showing the wave probes mounted on the wave flume	18
Photo. 3 Photograph showing the interface box and control box	18
Photo. 4 Photograph showing the storage oscilloscope and PC	19
Photo. 5 Photograph showing the wavemaker	19

LIST OF SYMBOLS

C. Phase velocity, m/s

C_g . Group velocity, m/s

C_o . Deep water phase velocity, m/s

d. Water depth (bed to SWL), m

E. Average energy density, N/m

f. Wave frequency, Hz

f_o . peak frequency, Hz

g. Gravitational acceleration, m^2/s

H_{o1} . Deep water wave height for probe 1, m

H_{o2} . Deep water wave height for probe 2, m

H_1 . Wave height for probe 1, m

H_2 . Wave height for probe 2, m

H_s . Significant wave height, m

K. Wave number, m^{-1}

K_{po} . Deep water wave number corresponding to peak frequency, m^{-1}

L. Wavelength, m

λ_o . Deep water wavelength, m

P. Energy flux, N/s

P_1 . Energy flux for probe 1, N/s

P_2 . Energy flux for probe 2, N/s

S, Spectrum, cm^2/s

T, Wave period, s

T_s , Significant wave period, s

U, Wind velocity, m/s

α , Philip's constant

γ , Peak enhancement factor

η_1 , Root mean square wave height for probe 1, m

η_2 , Root mean square wave height for probe 2, m

ε , Spectral width parameter

ω_p , Peak frequency, rad/sec

ω , Frequency, rad/sec

$\bar{\omega}$, Mean frequency, rad/sec

ρ , Density, Kg/m^3

Chapter I

INTRODUCTION

Offshore technology has experienced a remarkable growth in application in the recent years. At present a wide variety of offshore structures are being used even under severe environmental conditions. While these are predominantly related to oil and gas recovery, they are also being used in other applications such as harbour engineering and ocean thermal energy conversion. The potential of a major catastrophic failure, both in terms of human safety as well as economic loss, underlines the critical importance of efficient and reliable design.

The mechanism of transformation in shoaling of waves is a basic problem in coastal engineering. In fact, the action of waves is an important factor in the design of structures in the coastal and offshore zones. In traditional design irregularities of waves have not been taken into account directly. Irregular waves have been represented as a superposition of a few regular waves having a predetermined wave height and wave period.

The present thesis is concerned with the study of shoaling of regular and random waves. For regular waves, change in the characteristics of waves such as wave height and wave length as the waves propagate on a sloping beach have been studied. For random waves the following questions have been addressed.

- (i) Change in the power spectra with water depth.
- (ii) Change in dispersion relation of spectral components in shallow water conditions.
- (iii) Change in the relation between mean and peak frequencies of wave spectra propagating over sloping bottom.
- (iv) Variation of energy flux.

In parallel with studies of Bendykowska and Werner(1988) on the transformation of shallow water wave spectra, the present thesis is an experimental study of transformation of shallow water wave spectra.

The present thesis is organised along the following lines. Chapter II contains a review of the existing literature on wave shoaling. Chapter III describes experimental details including the equipments used, instrumentation and measurement. Results and discussion and conclusions are presented in Chapter V and VI, respectively.

Appendix A presents the measured signals in graphical form. Appendix B contains the definitions of important functions and parameters and their method of calculation. Appendix C contains computer programmes for calculating these quantities.

Chapter II

LITERATURE REVIEW

2.1 SHOALING OF REGULAR WAVES – As a wave train propagates into shallow water, its characteristics such as the wave height and wave length change. This process is described as wave shoaling. The shoaling effect may be estimated on the basis of a simplified linear wave theory. Commonly used assumptions for developing this theory are,

- (a) motion is two dimensional.
- (b) wave period remains constant.
- (c) energy flux in the direction of wave propagation is constant.

These assumptions require that sea bed has gentle slope resulting in negligible wave reflection and that energy be neither supplied nor dissipated by wave breaking or bottom roughness. The assumptions hold good only upto the point of breaking. Shoaling curves derived using assumptions given above show the variation of H / H_0 , $C / C_0 = (L / L_0)$ and C_g / C with $h / g T^2$ given by linear wave theory, are given in Figure 2.1. Relationship similar to those given above can be derived on the basis of a finite amplitude wave theory, but it is doubtful if a single wave theory will apply over the range

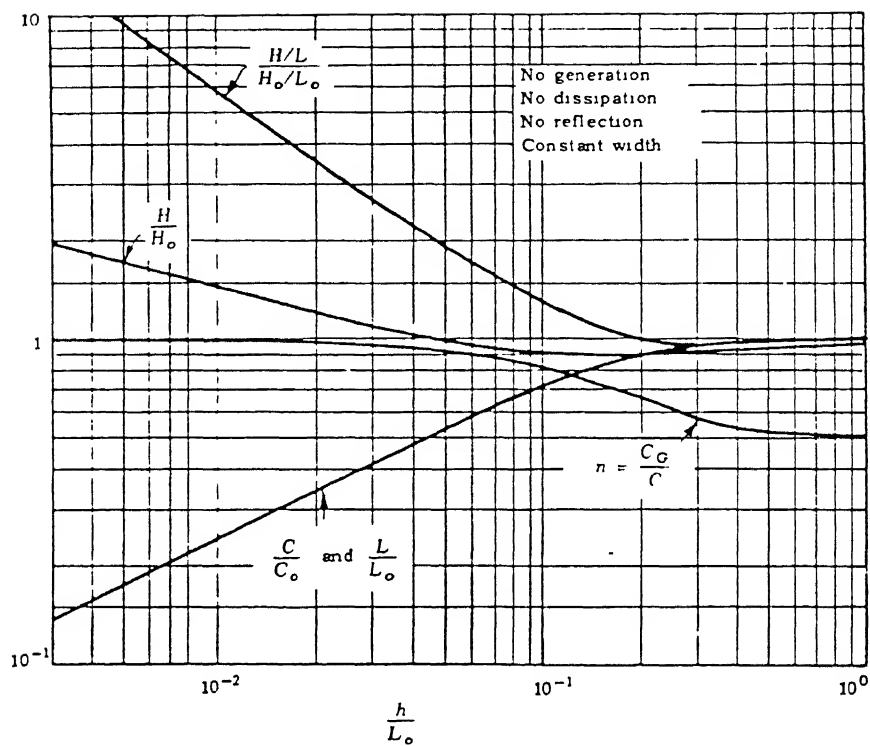


Fig. 2.1 Shoaling curves for regular waves

(Ippen, A. T.)

of depths, that cover deep water and shallow water.

Iversen (1952) presented experimental data that shows the height of periodic waves on sloping bottoms to grow faster than that predicted by sinusoidal wave theory. Harihar Rama Ayyar(1970) has studied the shoaling of regular waves in water over a steep bottom. The factors affecting the breakers characteristics are the incident wave steepness(H/gT^2) and bottom slope (m).

R. C. Nelson(1980) studied the effect of the bed slope on the characteristics of nonbreaking waves. The main results of his study are the following:

- (i) The characteristics of waves near breaking on a gentle slope cannot be same as those on a horizontal bed.
- (ii) The effect of bed slope of less than 0.1 on potential energy and wave celerity is minimal and for all practical purposes can be ignored.
- (iii) Bed slopes greater than or equal to 0.062 can significantly affect the ratio of crest height to wave height and trough depth to wave height.

Ib A. svendson & J. Buhr Hansen (1976) have studied the periodic waves moving on a beach and have compared the results with the theories of sinusoidal and cnoidal wave shoaling. Their results can be summarised as follows:

- (i) Linear theory can predict shoaling as long as wave height to water depth ratio is small.

(ii) At breaker point the wave length to water depth ratio appears to be independent of bottom slope for bottom slopes less than 1:10.

(iii) Phase velocity followed the prediction of linear wave theory for $h/L_o > 0.1$. Scattering may be present but can be attributed to small free secondary harmonic waves present in the flume.

(iv) Wave height discrepancy is attributed to friction of the walls of the flume.

2.2 MODELS FOR FREQUENCY SPECTRA — To study the random waves, mathematical models for wave spectra have been developed. These are in terms of a reference wind speed U appearing as a parameter. Of the following, Bretschneider and Pierson and Moskowitz spectra are most commonly used. JONSWAP spectra, an extension of the Pierson and Moskowitz spectrum produces a much sharper spectral peak, is more recent and involves additional parameters.

Pierson-Moskowitz Spectrum(1964)-This spectrum depends only on the wind speed and is given as.,

$$S(f) = \frac{\alpha g^2}{(2\pi)^4 f^5} \exp(-B/f^4)$$

Where $\alpha = 8.1 \times 10^{-3}$ and is termed as Philip's constant.
 B is $7.4(g/2\pi U)^4$

JONSWAP Spectrum (1973)- It is the modification to the Pierson-Moskowitz spectrum to account for the fetch restrictions and to provide a sharply peaked spectrum. It is given as,

$$S(f) = \frac{\alpha g^2}{(2\pi)^4 f^5} \exp \left[-\frac{5}{4} \left(\frac{f}{f_0} \right)^{-4} \right] \gamma^\alpha$$

$$\alpha = \exp \left[-(f-f_0)^2 / 2 \sigma^2 f^2 \right]$$

$$\sigma = \begin{cases} \sigma_a & \text{for } f \leq f_0 \\ \sigma_b & \text{for } f > f_0 \end{cases}$$

Here f_0 is peak frequency at which $S(f)$ is a maximum and is found to be related to fetch parameter as,

$$f_0 = 2.84 (gF^2/U^2)^{-0.22}$$

Parameters σ_a and σ_b relate respectively to the width of the left and right side of spectral peak.

α is Philip's constant and depends upon fetch parameter as,

$$\alpha = .066 (g F^2/U^2)^{-0.22}$$

2.3 SHOALING OF RANDOM WAVES -

The average rate of energy transfer per unit width, or energy flux, of a

unidirectional random wave train is given as,

$$P = \rho g \int_0^{\infty} C_g S(f) df$$

Where C_g is group velocity.

Thus transformation of a unidirectional spectrum during the wave shoaling is given by

$$C_g S(f) = \text{constant}$$

Testuo Sakai and Yuichi Iwagaki (1974) studied the transformation of random waves in shoaling water with the spectrum having one or two random peaks. It was found that the elementary peak power of random waves decreased with decrease in water depth. This reason can be explained qualitatively by theory of change of component wave height of finite amplitude waves in shoaling water. The damping due to internal viscosity and boundary friction was found to be negligible because it was of the same order of magnitude as the experimental error.

Bendykowska and Werner(1988) in their investigation on the shallow water wave spectra studied the effect of nonlinearity on shallow water wave spectra. The waves were generated mechanically in a laboratory wave flume with a fixed bottom. Deviation from linear dispersion relationship was found, showing a vanishing dispersivity of

higher frequency spectral components. The mean frequency was seen to increase with decreasing depth. The relation of peak frequency to mean frequency varied in experiments from 0.9 to 0.5 for deep and shallow water spectra respectively.

The main aim of present thesis is motivated by the work of Bendykowska and Werner(1988). However it is an independent study of the behaviour of regular and random waves as they move towards the shore.

Chapter III

EXPERIMENTAL DETAILS

3.1 EQUIPMENT

WAVEMAKER — The wavemaker is of the absorption type and comprises of following components. It has a flap which is wedge shaped paddle pivoted about its tapered end on a fabric hinge fixed to the bottom leading edge of the wavemaker box. The paddle is mounted in the box and extends the full width of the tank. The front of the box is sealed with a waterproof fabric gusset, behind which the paddle moves. This serves to prevent water entering the box with the result that the paddle operates only on the water in front of it. The paddle is driven by an electric servo-motor via a beryllium-copper drive belt which runs over a sector attached to the top of the paddle. The hydrostatic force on the flap is offset by springs. A piezo-electric transducer is sited between the sector and the paddle and senses the force acting on the

paddle. Position is sensed by an incremental encoder mounted on the motor-shaft.

CONTROL BOX — The control box contains the power amplifier for the wavemaker, along with the signal conditioning, force feedback, wave absorption and nonlinearity correction circuitry. There is also load protection circuit that disables the power amplifier under fault conditions.

An encoder on the drive motor is used for position sensing. The signals from this are counted, then converted to give analogue position signal. This is filtered to produce the velocity signals required to optimise the paddle absorption characteristics. The digital signal from the counter chain is passed to an EPROM that is programmed to provide a square law function for hydrodynamic and hydrostatic second order correction.

INTERFACE BOX — The interface box acts as the junction between the computer and outside world. All the signals to and from the interface card in the back of PC are run by a cable to the interface box. The inputs to this unit consist of 16 buffered analogue inputs with filters and four digital input circuits.

The analogue inputs can be independently viewed by switches in front panels. The outputs from the PC consist of two analogue signals for the wavemaker and four digital outputs. The wavemaking signals pass through a digital potentiometer to control the overall gain. Digital outputs are buffered by relays.

In addition, the interface box contains a sine wave generator for running the wavemaker without using the PC. The system is run by an internal power supply. The wavemaker control box returns force, velocity and drive signals that are available on a 15 way D connector on the rear of the interface box.

INTERFACE CARD — The interface card is manufactured by Advantech as part PCL 812 and plugs into an expansion slot of a PC. It provides two 12 bit analogue output channels, 16 analogue inputs, 16 digital inputs and 16 digital outputs.

WAVEGAUGE— This is a simple probe for sensing the elevation of water waves. It works on the principle of measuring the current flowing in a probe consisting of parallel stainless

steel wires. The probe is energised with a high frequency square wave voltage to avoid polarisation effects at the wire surface. The wire dips into water and current that flows between them is proportional to the depth of immersion. The current is sensed by an electronic circuit providing an output voltage proportional to the instantaneous depth of immersion and hence wave height. It can be used to drive a high speed chart recorder and/or a data logger.

The standard form of the probe consists of a pair of stainless steel wire, 1.5 mm in diameter and spaced 12.5 mm apart. However flexibility of drive and sensing circuits enables a wide variety of probe configuration to be employed.

The output voltage can be calibrated in terms of wave height by varying the depth of immersion of probe in still water by a measured amount and noting the change in the output signal. A special probe support member with accurately spaced positioning holes is available to facilitate this operation.

The photographs of the equipments used in the present study are given in Photograph 1 to 5.

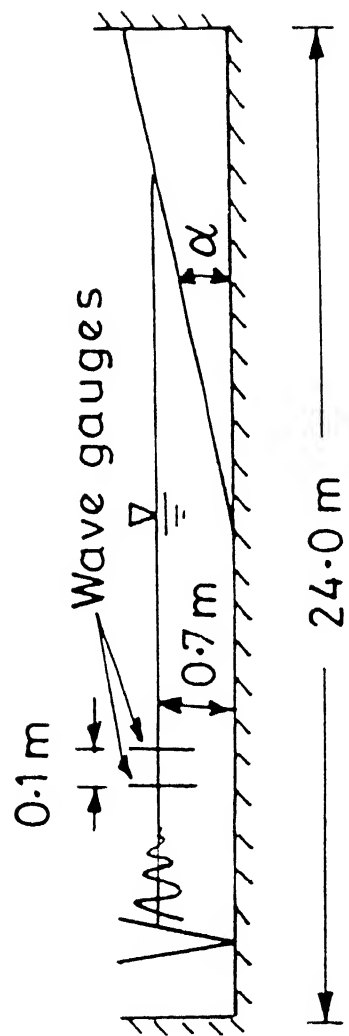


Fig. 3.1 A Schematic Illustration of Wave Flume

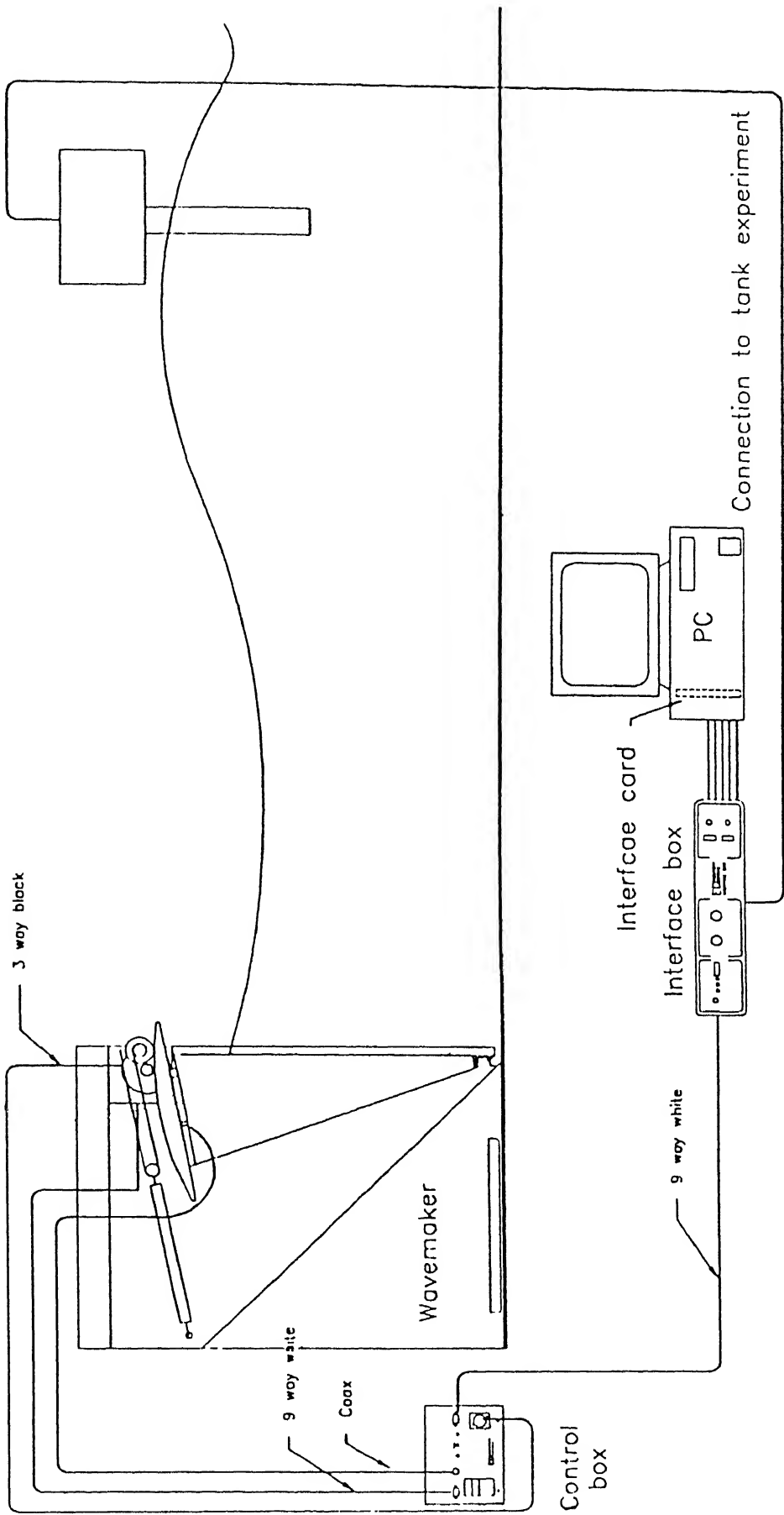


Fig. 3.2 A Schematic Illustration of Wavemaker

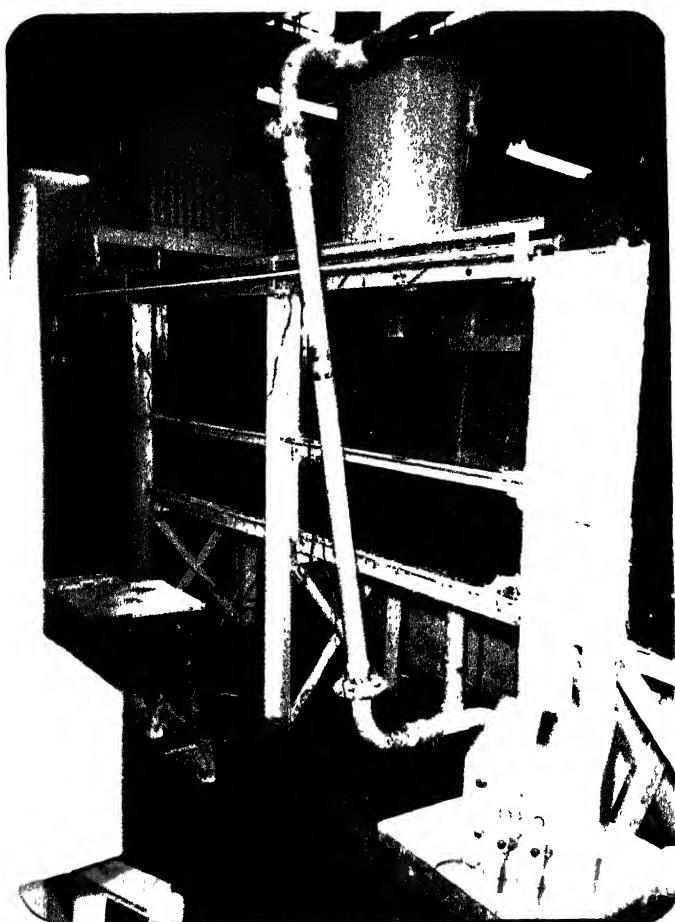


Photo. 1 Photograph showing the wave flume
with piping for filling and emptying
the wave flume and wave monitor

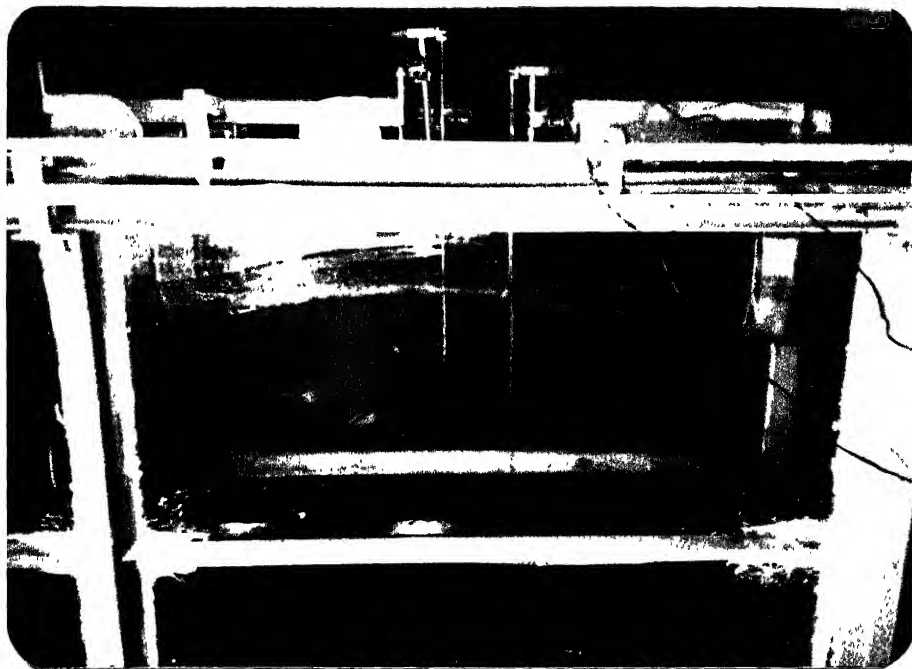


Photo. 2 Photograph showing the wave probes
mounted on the wave flume

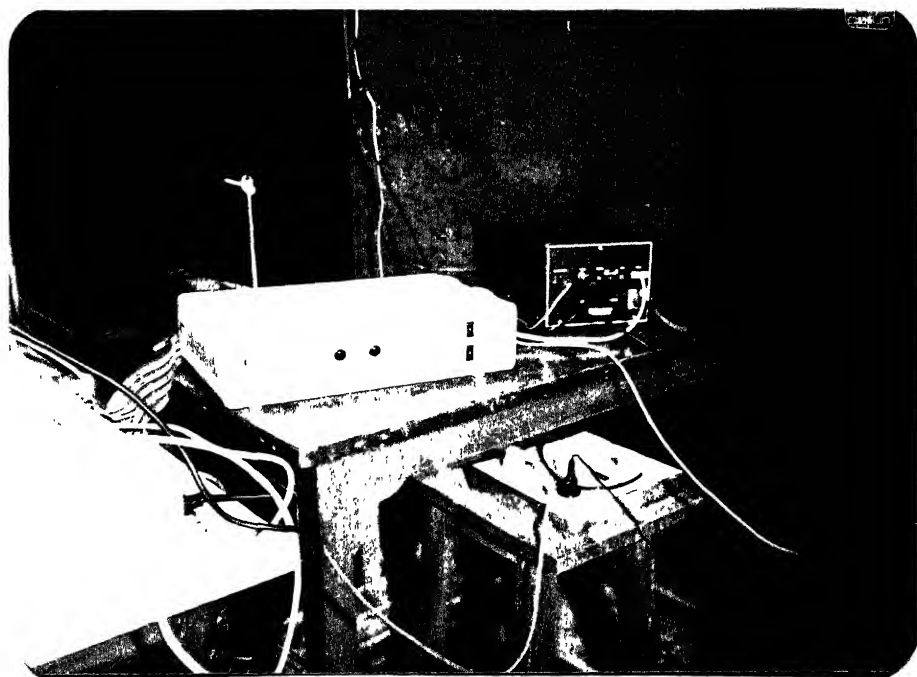


Photo. 3 Photograph showing the interface box
and control box



Photo. 4 Photograph showing the storage
oscilloscope and PC



Photo. 5 Photograph showing the wavemaker

3.2 SPECIFICATIONS-

3.2.1 OSCILLOSCOPE

Model number	: HP 54501 A Digitizing oscilloscope
Manufacture	: Hewllett Packard
Number of input channels	: 4
Input coupling	: AC , DC
Storage mode	: Oscilloscope digitizes the input signal before displaying the trace
Normal mode	: Behaves like a conventional analog instrument
Vertical sensitivity	: Maximum 5 mv/div Minimum 5 v/div
Vertical gain accuracy (dc)	: + 1.5 %
Time base accuracy	: 0.005 %
Time base range	: 2 ns/div to 5 s/div
Maximum sample rate	: 10 Ms/s
Memory depth	: 501 Points (display) 1024 Points (via HP-IB)
Signal averaging	: 1 to 1024

3.2.2 PC

Type	: 386 SX
Manufacturer	: WIPRO (PVT) Ltd, Bangalore

3.2.3 INTERFACE CARD

Model	: PCL 812
-------	-----------

3.2.4 WAVE GAUGE AND MONITOR

Type : Capacitance
 Manufacturer : Armfield Ltd, U.K.
 Output voltage : \pm 10 volt
 Range : 500 mm
 Frequency response : 10 Hz

3.2.5 WAVEMAKER

Type : Absorption wavemaker
 Manufacturer : C & N Electrical Industries
 Ltd, England.
 Component parts : (a) Paddle assembly
 (b) Hinge
 (c) Membrane seal
 (d) Coupling wire
 (e) Spring
 (f) Anchor chord
 (g) Motor tacho
 (h) P.C.B.(Contrl board)
 Power supply : +7.5 V and -7.5 V, 250 ma and
 +15 V and -15 V, 10 Amp per
 paddle system

3.3 PROCEDURE

Experiments were conducted in a wave flume which is 24 meters long, 0.45 meter wide and 0.90 meter deep. A wave generator of flap-hinge type was installed at one end of the flume. A uniform sloping beach was set in the flume. This beach was made out of aluminium plates. The slope of the beach was 1 / 20. A schematic sketch of the wave flume is given in Figure 3.1 . In all experiments water depth in the constant depth region was kept at 70 cm. Positions of PC, interface box and control box were connected as given in the Figure 3.2.

First of all, wavegauge was calibrated by raising or lowering it by a known amount in still water. This operation was facilitated by mean of a calibrated holder which has series of holes drilled along its length, accurately spaced at 10 mm. The probe was raised or lowered by a multiple of 10 mm by using the pin provided as a stop.

After calibrating the probe, regular and random waves with a JONSWAP spectrum were generated by PC using the computer programmes given in Appendix C. For regular waves, data was collected at 10 places in constant water depth and at 80 cm interval on the slope upto a depth of 5 cm. For random waves, experiments were conducted for three different cases. These cases are described in Table 3.1. Data

was collected at four locations in constant water depth and at 1 meter interval on the slope upto a depth of 5 cm.

Regular waves were generated with 1 Hz frequency and 5 cm amplitude. Three JONSWAP spectra waves were generated with a peak frequency of 1 Hz, 0.75 Hz and 0.60 Hz and peak enhancement factor of 6.0, 1.0, and 1.0 respectively.

The signals were collected by the PC in terms of voltages. These were converted to water surface elevation by using the calibration curve.

Spectral analysis of the water surface elevation signal was performed by using FFT software on HP main-frame computer. The phase difference ϕ between signals of the two probes was obtained from cross spectral analysis. This phase difference was used to determine the wave number and celerity. Data having the cross correlation coefficient factor of greater than 0.8 has been identified as acceptable. Group velocity and energy flux for regular waves were calculated by using small amplitude wave theory.

Table 3.1 PARAMETERS OF JONSWAP SPECTRA

$$S(f) = \frac{\alpha g^2}{(2\pi)^4 f^5} \exp \left[-\frac{5}{4} \left(\frac{f}{f_0} \right)^{-4} \right] \gamma^\alpha$$

Where

$$\alpha = \exp \left[- (f - f_0)^2 / 2\sigma^2 f_0^2 \right]$$

$$\sigma = \begin{cases} \sigma_a = 0.07 & \text{for } f \leq f_0 \\ \sigma_b = 0.09 & \text{for } f > f_0 \end{cases}$$

$$g = 9.81 \text{ m/s}^2, \quad \alpha = \text{Philip's constant} = 0.0081$$

	f_0 (Hz)	γ
CASE 1	1.00	6.0
CASE 2	0.75	1.0
CASE 3	0.60	1.0

Chapter IV

RESULTS AND DISCUSSION

Results have been presented separately for regular and random waves.

REGULAR WAVES-

Wave height and root mean square wave height have been tabulated in Table 4.1. Figure 4.1 shows the recorded variation of wave height as a function of the local depth parameter h/L_o for a deep water steepness $H_o/L_o = 0.055$. It can be observed that the wave height decreases as the depth of water decreases. The experimental data follows the small amplitude wave theory for h/L_o larger than 0.15. For $h/L_o < 0.15$, experimental data does not follow the small amplitude wave theory.

The dimensionless phase velocity, group velocity normalised by phase velocity and energy flux are given in Table 4.2. The variation of dimensionless phase velocity and C_g/C with the dimensionless depth h/L_o are shown in Figure 4.2 and Figure 4.3 respectively. The data is seen to follow the trend predicted by small amplitude wave theory. The variation of C_g/C with h/L_o shows that this increases as the water depth

decreases. Figure 4.5 shows the variation of the energy flux with water depth. Energy flux is seen to decrease with decreasing depth. This is against the assumption of a constant energy flux used in small amplitude theory.

The deviation of experimental results from theoretical predictions can be attributed to the following factor.

Propagation of energy flux to the water below the beach. It is believed that this factor is the most significant one.

RANDOM WAVES-

Cross-spectral analysis was applied to two simultaneous records taken 10 cm apart. Wave numbers $K(\omega)$ and celerity $C(\omega)$ of the spectral components for each frequency were determined. The effect of nonlinearity was examined by varying the peak frequency of JONSWAP spectra in the range of $3.76 \leq \omega_p \leq 6.28$ (rad/sec) at different water depths.

Power spectra of wave heights measured at different depths are presented in Figure 4.6 to Figure 4.8. There is a substantial drop in spectral peak. This shows the increasing nonlinearity of wave motion at small depths. Figure 4.6 to Figure 4.8 explain the increasing nonlinearity of wave motion on small depth.

Figure 4.9 to Figure 4.12 show a comprehensive plot of

wave height spectra for the three cases summarised in Table 3.1. Results have been shown in constant depth region followed by the spectra for variable depth portion of the flume. The plots are practically identical in constant depth region. As one moves over the slope, wave having a given value of γ develop an increase in spectral peak with decrease in peak frequency.

From Figure 4.13 to Figure 4.16 results of wave frequency ω against the wave number K with the theoretical curve are plotted. All measured results indicate that the prediction of linear theory are true only in the vicinity of peak frequency. but as the depth of water decreases nonlinearity also increases because we get more deviation from the theoretical curve.

From Figure 4.17 to Figure 4.19 the line $C(\omega)/C_0(\omega)=1$ is the theoretical relation. The phase velocity in range $\omega_p < \omega < 2\omega_p$ follows the theoretical curve. Most of spectral components of $\omega > 2\omega_p$ travel at higher velocity than the theoretical. The presence of bounded wave is one of the explanation. Same results are obtained by Crawford et al in 1981 in their numerical study.

Results concerning the changes of mean frequency of the spectrum, when propagating from deep water (ω_0) over decreasing depth ω are shown in Figure 4.20. This figure shows an increase of mean frequency when water depth decreases.

Changes of relationship between the peak ω_p and the mean frequency $\bar{\omega}$ of the spectrum as the function of relative water depth $K_{po} \cdot h$ ($K_{po} = \omega_p^2/g$) is given in Figure 4.21. The relation $\omega_p/\bar{\omega}$ varies from 0.5 on deep water to 0.2 for very small relative depth. These changes are due to change of the shape of the spectra.

Table 4.3 to Table 4.5 show energy flux, spectrum width parameter and coherence factor. The coherence factor is quite high (greater than 0.8) in majority of experiments. Spectral width parameter is about 0.9 in all experiments, showing that generated random waves are practically Gaussian. The energy flux calculations employ the experimental wave height spectra. Wave number calculated on the basis of the dispersion relation produce the column of energy flux marked Theor. Energy flux corresponding to peak frequency is marked $P(\omega_p)$ and that averaged over the range $0 \geq \omega_p \geq 3$ is marked $P(ave)$. The experimental energy flux calculation employs experimentally determined values of the wave number. These calculations show the energy flux to behave erratically and has not been used for analysis. The theoretical values ($P(Theor)$) show a reduction in energy flux over the beach. This is most prominent for depths less than 37.5 cms. As in the case of regular waves, this is attributed to the propagation of the energy flux to the water below the beach.

Table 4.1 calculation of wave height and r. m. s. wave height for regular waves

$$H_{o1} = 8.34 \text{ cm}, H_{o2} = 9.18 \text{ cm} \quad f = 1.0 \text{ Hz}$$

S. No.	distance from wave- maker (m)	d/L_o	H_1/H_{o1}	H_2/H_{o2}	η_1/H_{o1}	η_2/H_{o2}
1	4.0	0.4487	0.9846	0.9846	0.349	0.337
2	5.0	0.4326	1.0190	0.9836	0.340	0.334
3	5.8	0.4075	1.0770	1.0570	0.365	0.356
4	6.6	0.3814	0.9832	0.9771	0.340	0.337
5	7.4	0.3557	0.9520	0.9705	0.331	0.342
6	8.2	0.3301	0.9580	0.9564	0.330	0.328
7	9.0	0.3044	0.9221	0.9117	0.316	0.313
8	9.8	0.2788	0.9410	0.9204	0.316	0.313
9	10.6	0.2532	0.9377	0.8856	0.323	0.305
10	11.4	0.2275	0.9017	0.8801	0.310	0.301
11	12.2	0.2019	0.8934	0.8447	0.351	0.288
12	13.0	0.1762	0.8742	0.8137	0.286	0.274
13	13.8	0.1506	0.8038	0.7581	0.286	0.264
14	14.2	0.1250	0.7775	0.8000	0.251	0.263
15	15.0	0.0993	0.7341	0.7603	0.255	0.260
16	15.4	0.0865	0.7440	0.7734	0.242	0.268
17	15.8	0.0737	0.7544	0.7309	0.228	0.231
18	16.2	0.0608	0.6814	0.5577	0.215	0.202
19	16.6	0.0480	0.5389	0.4117	0.195	0.167
20	17.0	0.0352	0.6241	0.5034	0.163	0.134

Table 4.2 Calculation of C/C_0 , C/C_g , P_1 and P_2
for regular waves

$$C_0 = L_0 = 1.56 \text{ meter}$$

$$f = 1.0 \text{ Hz}$$

S. No.	distance from wave- maker (m)	d/L_0	C/C_g	C/C_0	P_1 (N/ Sec)	P_2 (N/ Sec)
1	4.0	0.4487	0.511	0.8910	5.90	7.12
2	5.0	0.4326	0.513	0.8884	6.27	7.06
3	5.8	0.4075	0.516	0.8717	6.96	8.10
4	6.6	0.3814	0.517	0.8269	5.50	6.56
5	7.4	0.3557	0.526	0.8397	5.33	6.70
6	8.2	0.3301	0.532	0.8205	5.33	6.42
7	9.0	0.3044	0.538	0.7884	4.80	6.24
8	9.8	0.2788	0.559	0.8141	4.99	6.19
9	10.6	0.2532	0.584	0.8333	5.70	6.14
10	11.4	0.2275	0.569	0.6987	4.30	4.96
11	13.0	0.1762	0.655	0.7500	5.00	5.73
12	13.8	0.1506	0.634	0.6000	3.27	3.51
13	14.6	0.1250	0.735	0.6858	4.05	5.18
14	15.0	0.0993	0.767	0.6070	3.33	4.30
15	15.4	0.0890	0.795	0.5814	3.31	4.27
16	15.8	0.0737	0.868	0.6600	4.21	4.96

Table 4.3 Calculation of coherence factor, spectrum width parameter and energy flux for random waves (CASE 1)

S. No.	distance from the wavemaker (m)	depth of water (cm)	coher- ence factor	ϵ	$P(\omega_p)$ N/sec. (TheorY)	$P(\text{ave})$ N/sec. (TheorY)	$P(\omega_p)$ N/sec. (Exp.)	$P(\text{ave})$ N/sec. (Exp.)
1	2.5	70.0	0.80	0.90	2.60	1.13	0.05	0.513
2	3.0	70.0	0.81	0.90	2.64	1.13	0.15	0.048
3	3.5	70.0	0.79	0.90	2.65	1.12	2.24	0.994
4	4.0	70.0	0.84	0.90	2.67	1.12	0.15	0.085
5	5.0	67.5	0.81	0.88	2.53	1.07	2.43	1.410
6	6.0	62.5	0.81	0.90	2.53	1.07	0.08	0.401
7	7.0	57.5	0.83	0.88	2.35	1.01	0.08	0.071
8	8.0	52.5	0.81	0.90	2.25	0.94	2.45	1.060
9	9.0	47.5	0.80	0.88	2.12	0.87	0.15	0.084
10	10.0	42.5	0.82	0.88	1.87	0.80	2.67	0.989
11	11.0	37.5	0.84	0.88	1.65	0.72	2.91	1.110
12	12.0	32.5	0.79	0.87	1.58	0.64	0.70	0.163
13	13.0	27.5	0.81	0.87	1.30	0.54	2.60	1.030
14	14.0	22.5	0.72	0.87	1.07	0.44	0.07	0.075
15	15.5	15.0	0.67	0.87	0.62	0.30	0.12	0.257
16	16.0	12.5	0.98	0.88	0.59	0.25	1.67	0.690
17	16.5	10.0	0.98	0.90	0.46	0.20	1.80	0.794

Table 4.4 Calculation of coherence factor, spectrum width parameter and energy flux for random waves (CASE 2)

S. No.	distance from the wavemaker (m)	depth of water (cm)	coher- ence factor	ϵ	$P(\omega_p)$ N/sec. (Theor.)	$P(\text{ave})$ N/sec. (Theor.)	$P(\omega_p)$ N/sec. (Exp.)	$P(\text{ave})$ N/sec. (Exp.)
1	2.5	70.0	0.85	0.92	2.19	1.86	0.09	0.185
2	3.0	70.0	0.86	0.92	2.33	1.91	0.08	0.204
3	3.5	70.0	0.85	0.92	2.18	1.89	1.92	1.57
4	4.0	70.0	0.88	0.92	2.33	1.90	0.07	.205
5	5.0	67.5	0.86	0.91	2.24	1.83	2.19	1.70
6	6.0	62.5	0.86	0.92	2.13	1.83	2.00	1.60
7	7.0	57.5	0.87	0.91	2.01	1.76	0.09	0.08
8	8.0	52.5	0.85	0.91	1.92	1.61	0.09	0.131
9	9.0	47.5	0.85	0.91	1.89	1.51	0.06	0.233
10	10.0	42.5	0.86	0.91	1.63	1.35	1.96	1.660
11	11.0	37.5	0.86	0.91	1.41	1.19	2.03	1.780
12	12.0	32.5	0.83	0.91	1.19	1.06	0.10	0.183
13	13.0	27.5	0.84	0.90	1.00	0.879	1.84	1.500
14	14.0	22.5	0.76	0.90	0.81	0.703	0.03	0.126
15	15.0	17.5	0.74	0.90	0.58	0.554	0.06	0.197
16	15.5	15.0	0.73	0.90	0.58	0.474	1.26	1.060
17	16.0	12.5	0.98	0.91	0.44	0.389	0.07	0.370
18	16.5	10.0	0.98	0.91	0.35	0.318	0.07	0.385

Table 4.5 Calculation of coherence factor, spectrum width parameter and energy flux for random waves (CASE 3)

S. No.	distance from the wavemaker (m)	depth of water (cm)	coher- ence factor	ϵ	$P(\omega_p)$ N/sec. (Theory)	$P(\text{ave})$ N/sec. (Theory)	$P(\omega_p)$ N/sec. (Exp.)	$P(\text{ave})$ N/sec. (Exp.)
1	2.5	70.0	0.91	0.94	4.20	3.040	4.78	2.660
2	3.0	70.0	0.91	0.94	4.60	3.060	0.04	0.214
3	3.5	70.0	0.79	0.93	1.98	2.030	1.09	1.830
4	4.0	70.0	0.93	0.94	4.16	3.080	0.09	0.311
5	5.0	67.5	0.92	0.94	4.57	2.980	5.24	3.721
6	6.0	62.5	0.91	0.94	4.02	2.950	3.72	4.962
7	7.0	57.5	0.92	0.94	4.52	2.870	5.83	2.640
8	8.0	52.5	0.91	0.93	3.42	2.610	3.06	2.546
9	9.0	47.5	0.91	0.93	3.47	2.450	0.03	0.356
10	10.0	42.5	0.91	0.93	3.02	2.200	0.07	0.033
11	11.0	37.5	0.90	0.93	2.43	1.910	0.08	0.387
12	12.0	32.5	0.88	0.93	2.31	1.710	0.03	0.059
13	13.0	27.5	0.89	0.93	1.88	1.460	2.57	3.660
14	14.0	22.5	0.82	0.93	1.49	1.150	1.83	1.540
15	15.0	17.5	0.82	0.93	1.10	0.890	1.52	1.530
16	15.5	15.0	0.79	0.93	0.69	0.772	1.76	2.322
17	16.0	12.5	0.97	0.94	0.68	0.606	0.03	0.328
18	16.5	10.0	0.97	0.94	0.29	0.450	0.18	0.298

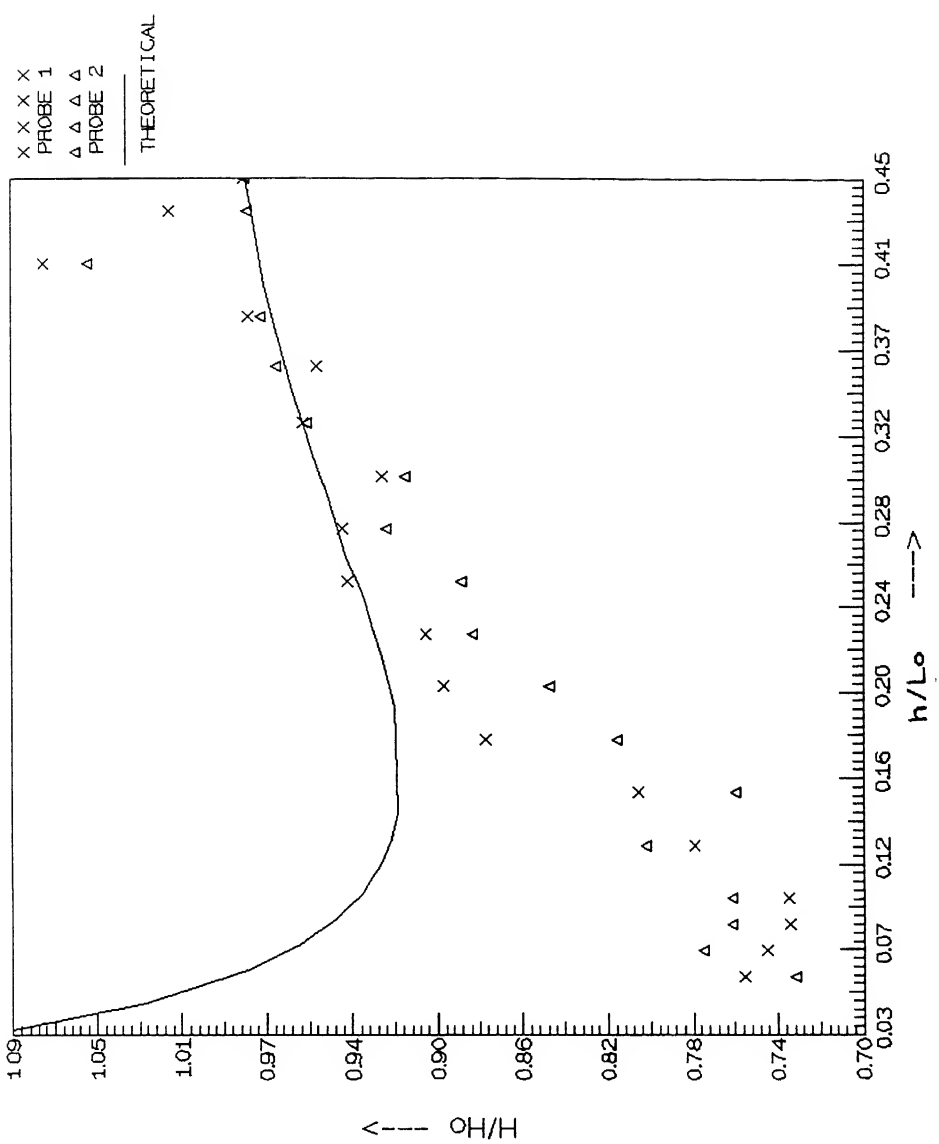


Fig. 4.1 H/H_0 versus h/L_0 for regular waves

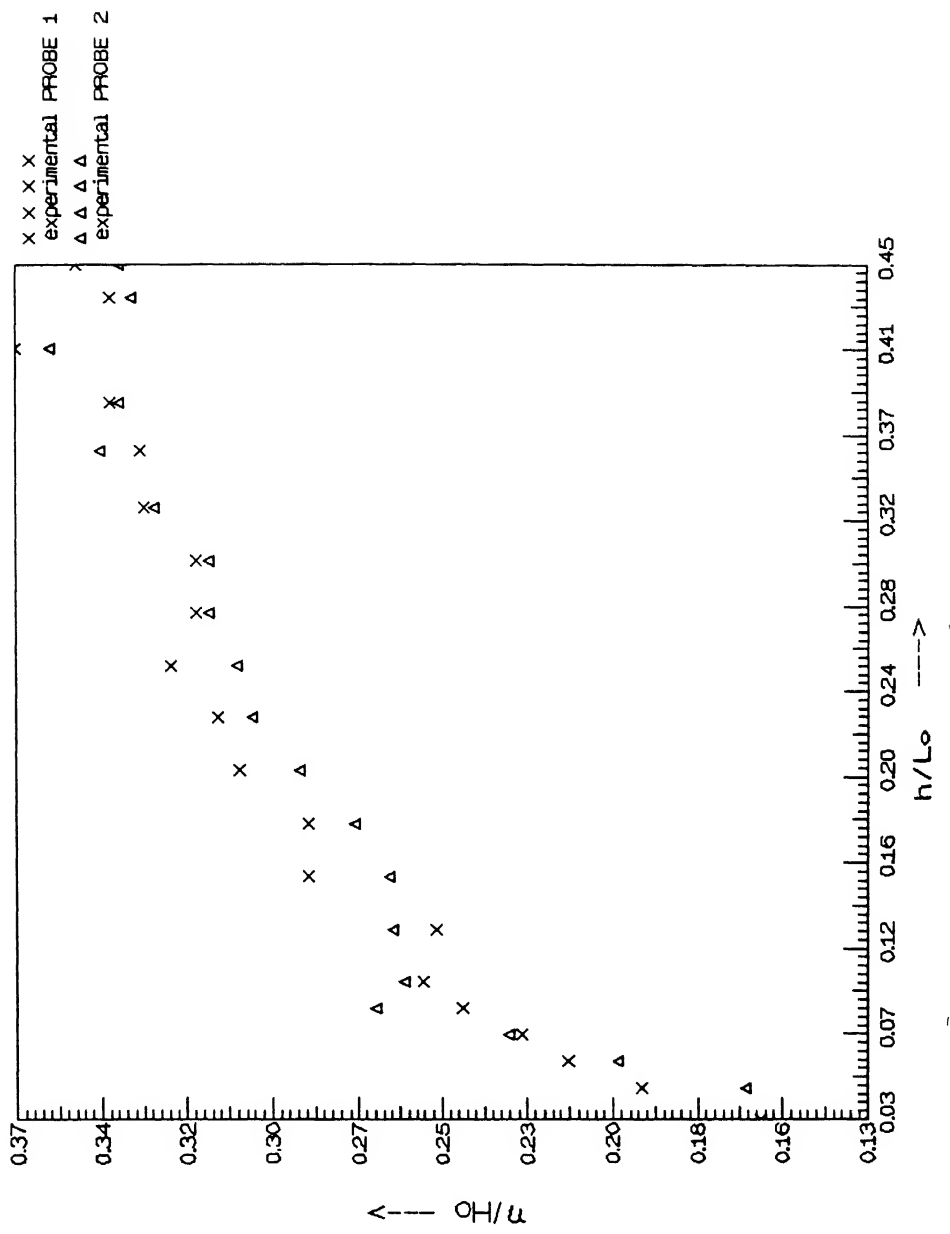


Fig. 4.2 η / H_0 versus h / L_0 for regular waves

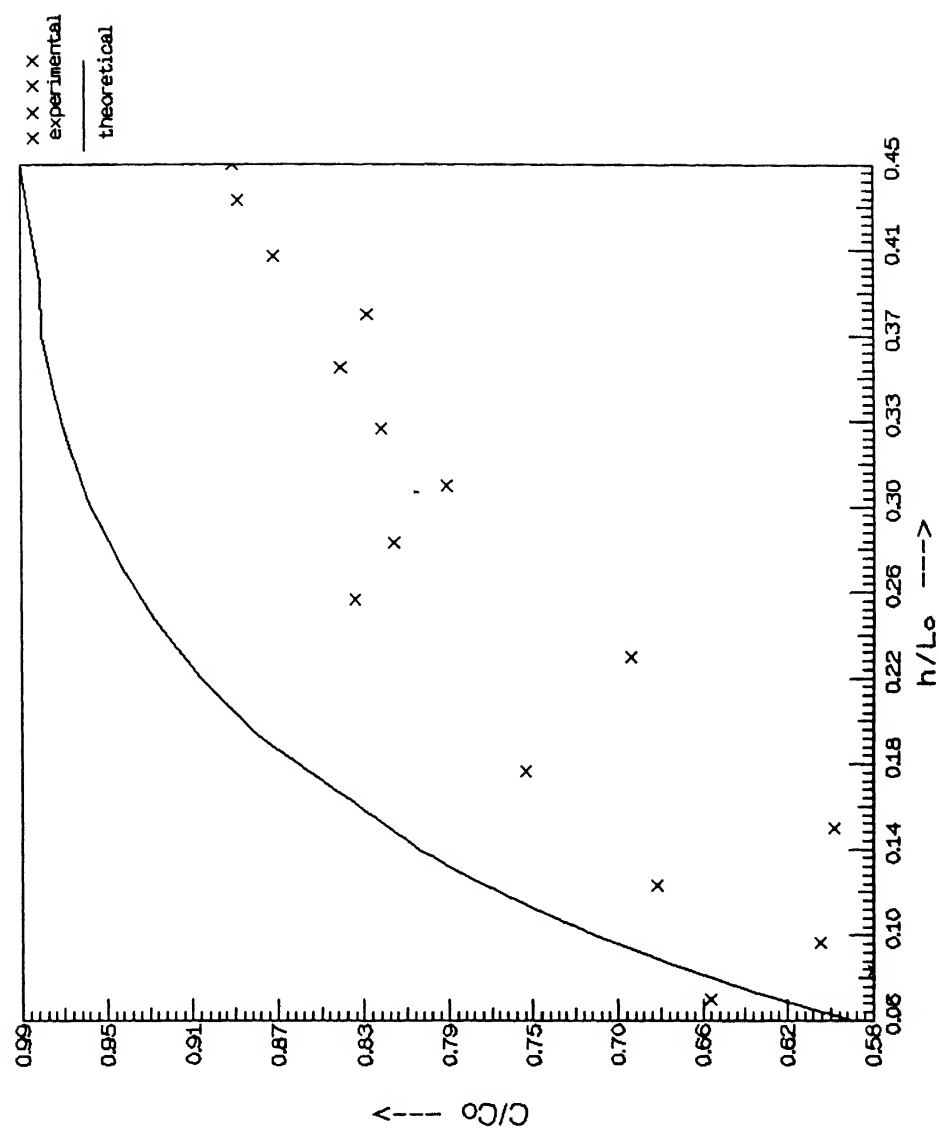


Fig. 4.3 C/C_0 versus h/L_0 for regular waves

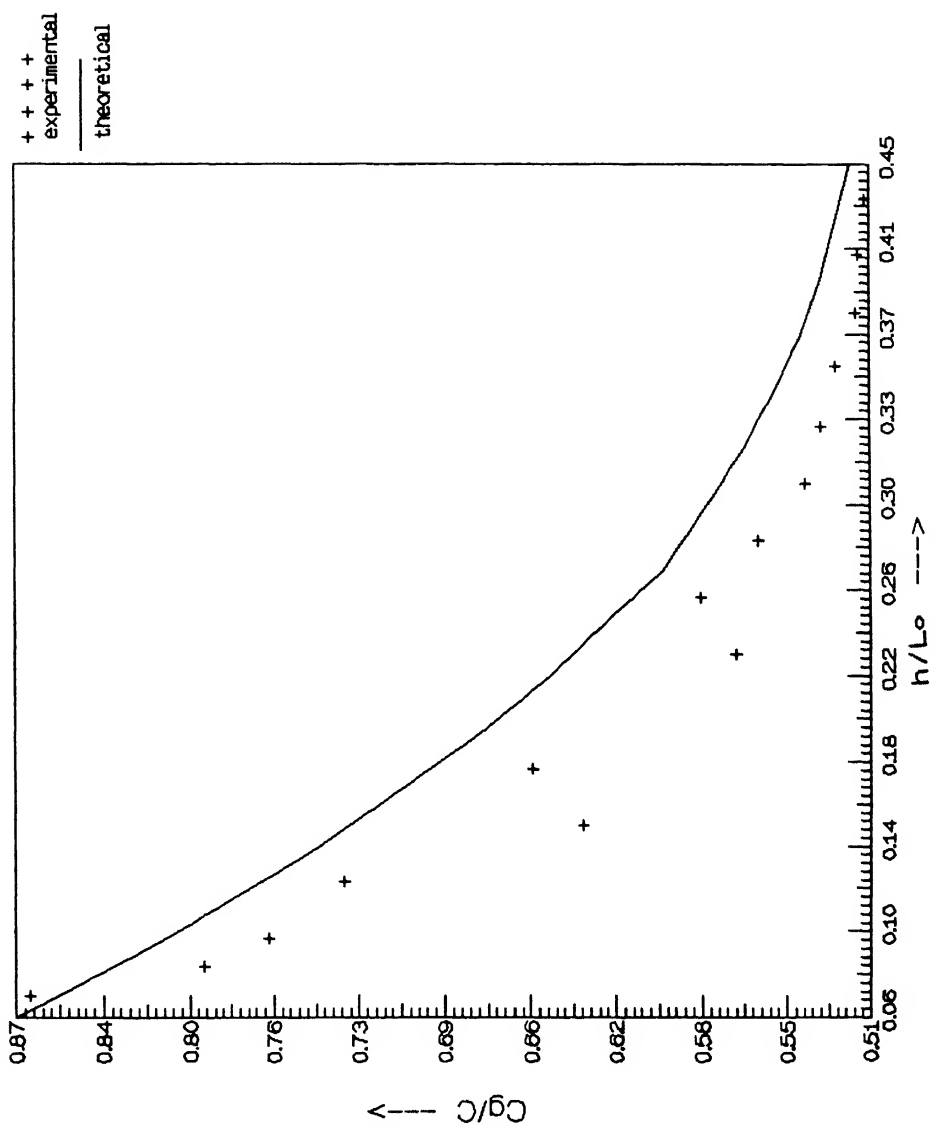


Fig. 4.4 C_g/C versus h/L_o for regular waves

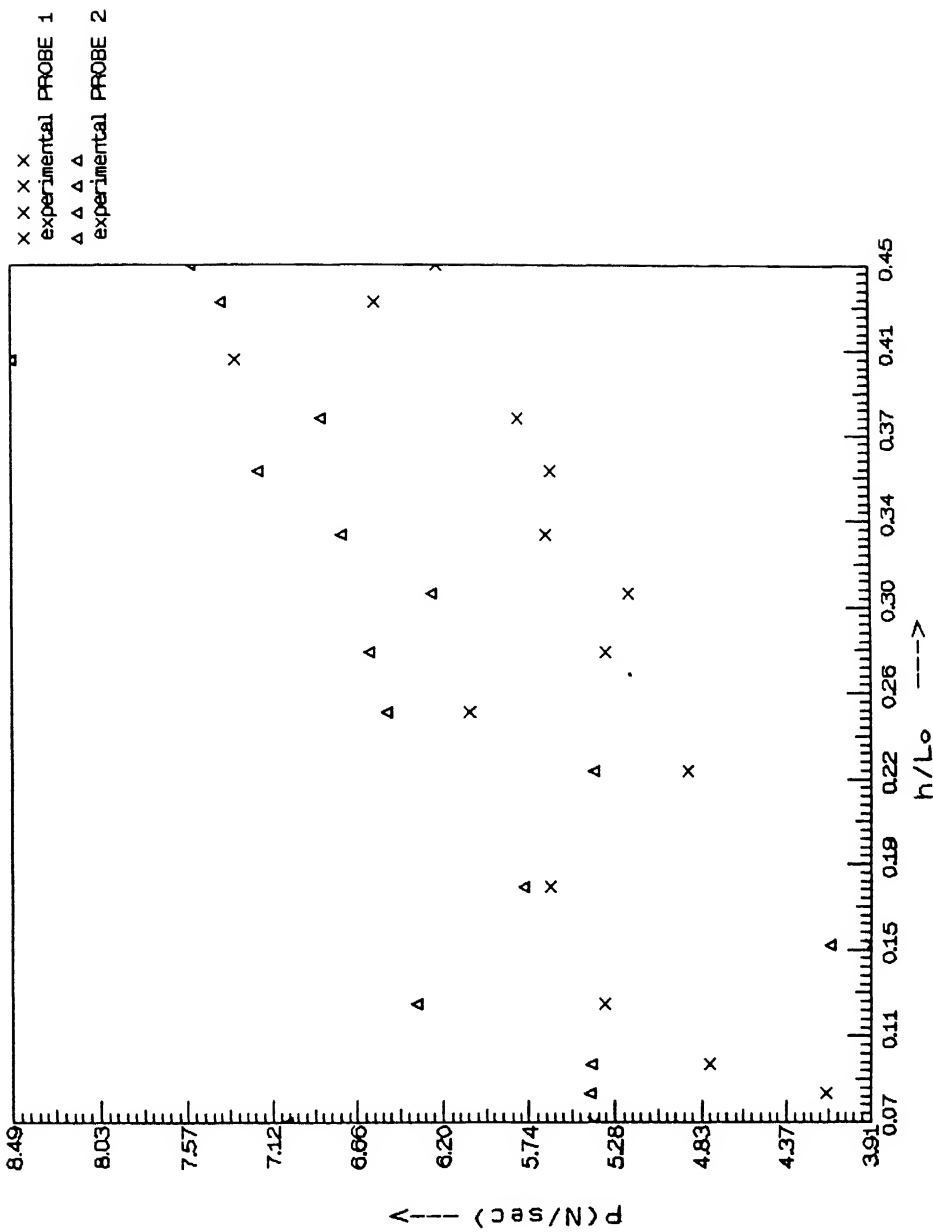


Fig. 4.5 P versus h/L_o for regular waves

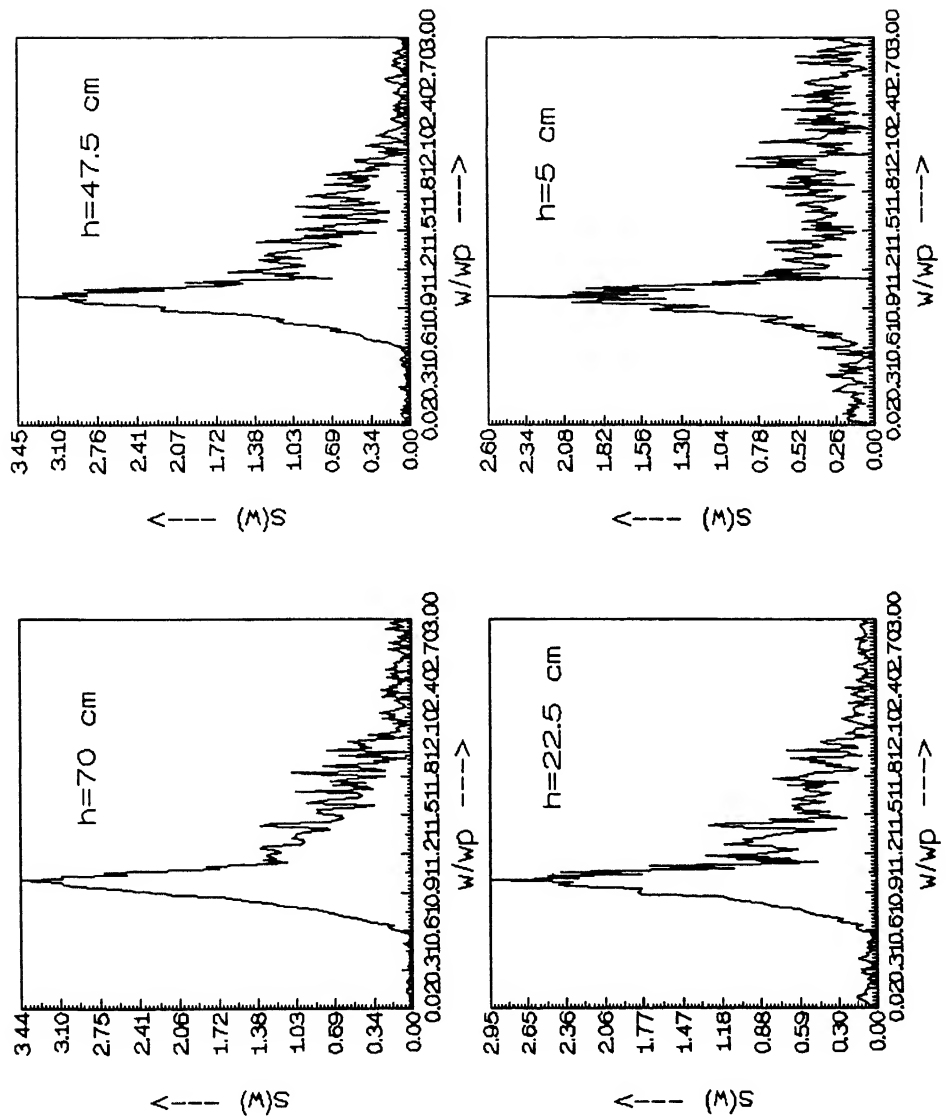


Fig. 4.6 $S(\omega)$ versus w/w_p for different water depths (CASE 1)

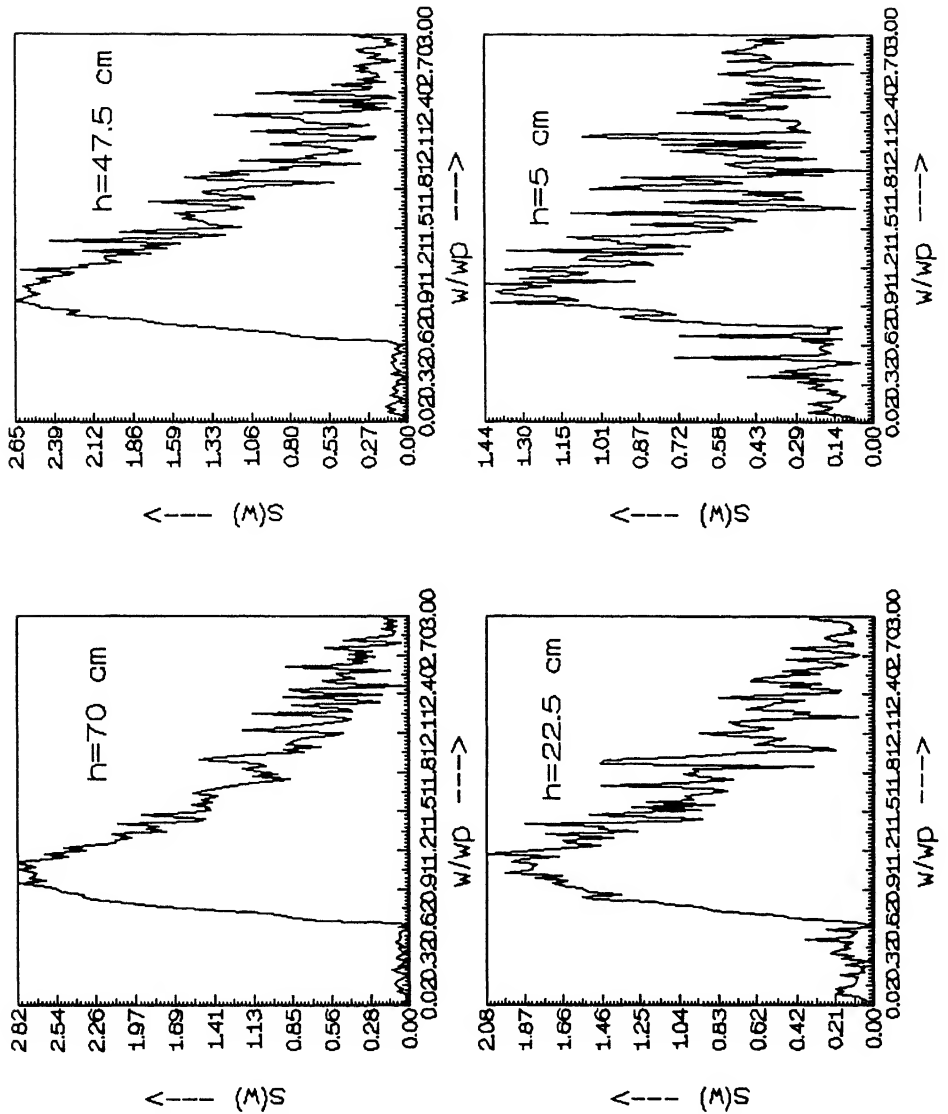


Fig. 4.7 $S(\omega)$ versus ω/ω_p for different water depths (CASE 2)

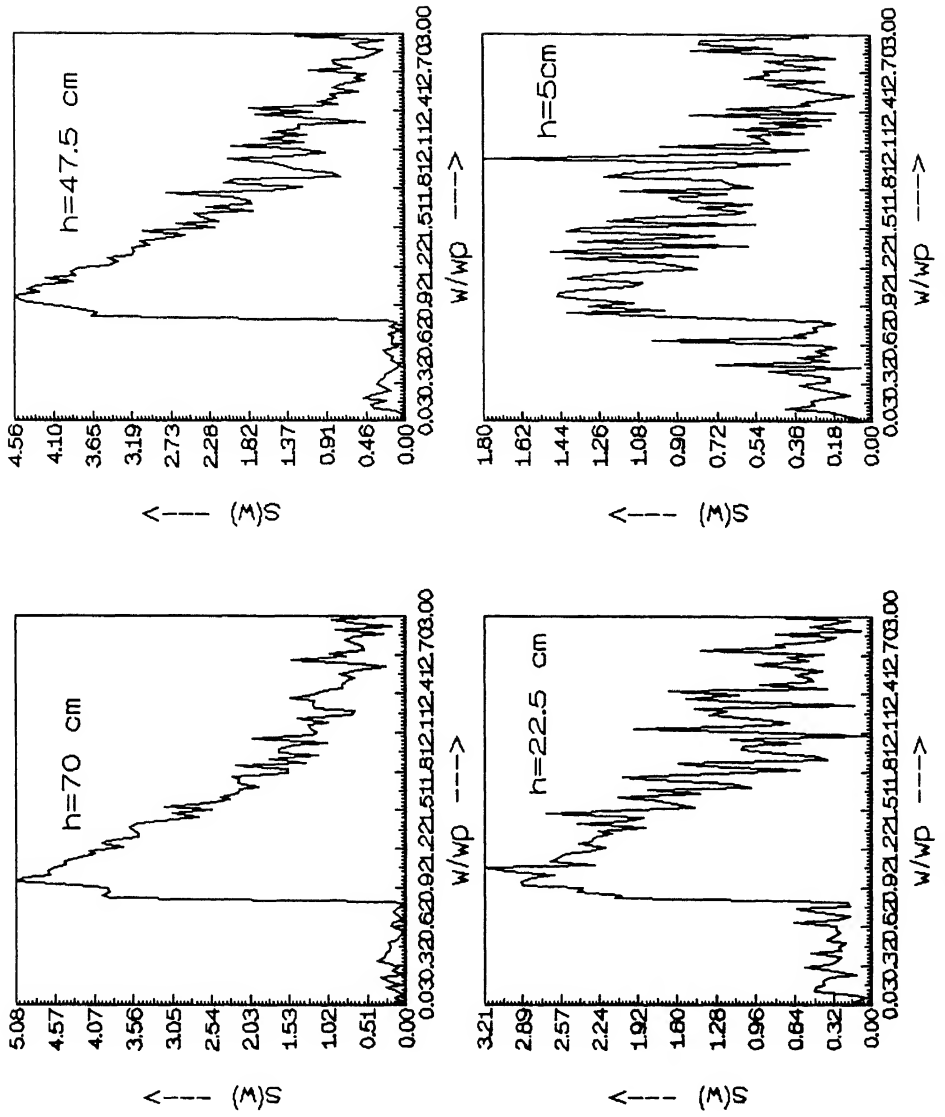


Fig. 4.8 $S(\omega)$ versus ω/ω_p for different water depths (CASE 3)

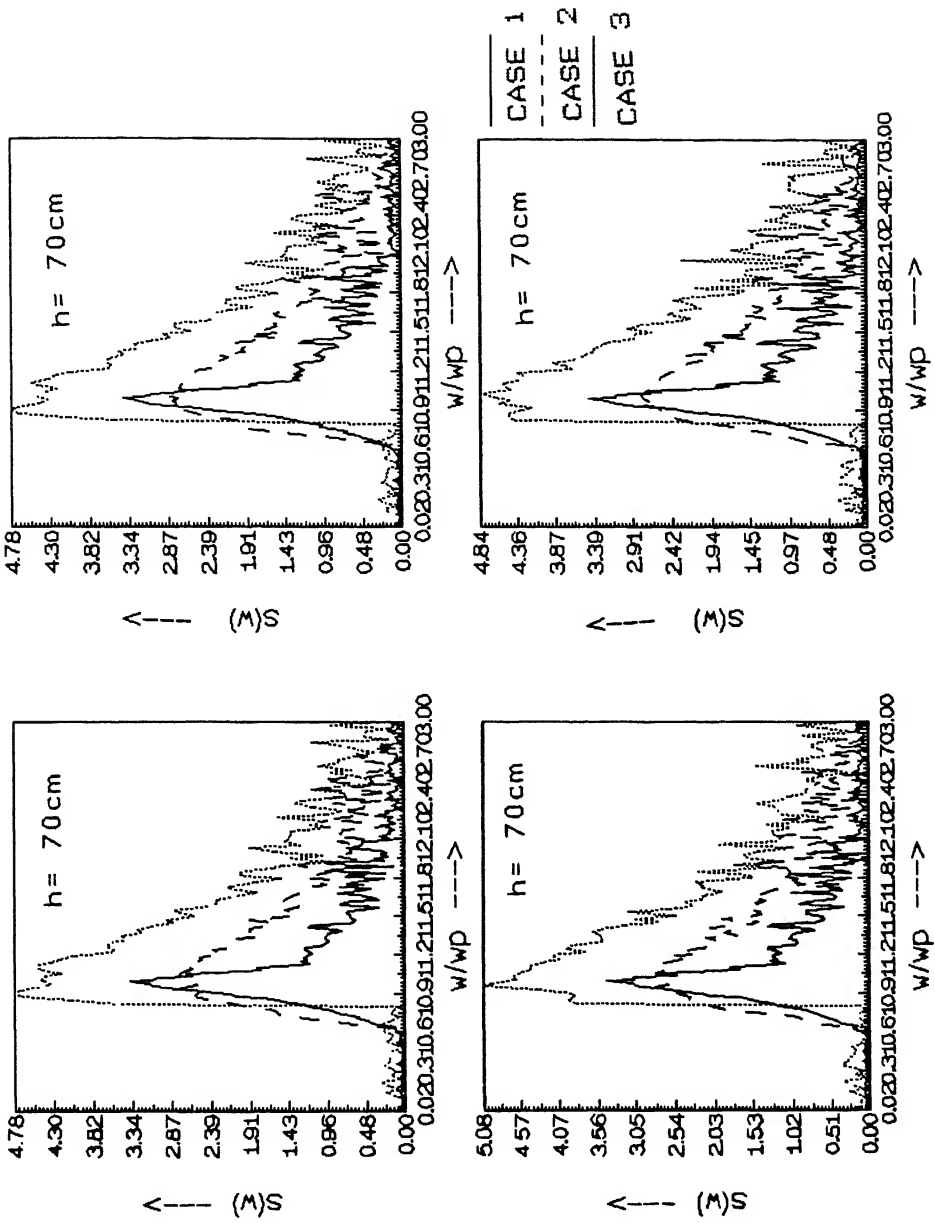


Fig. 4.9 $S(\omega)$ versus ω/ω_p for $h = 70 \text{ cm}$

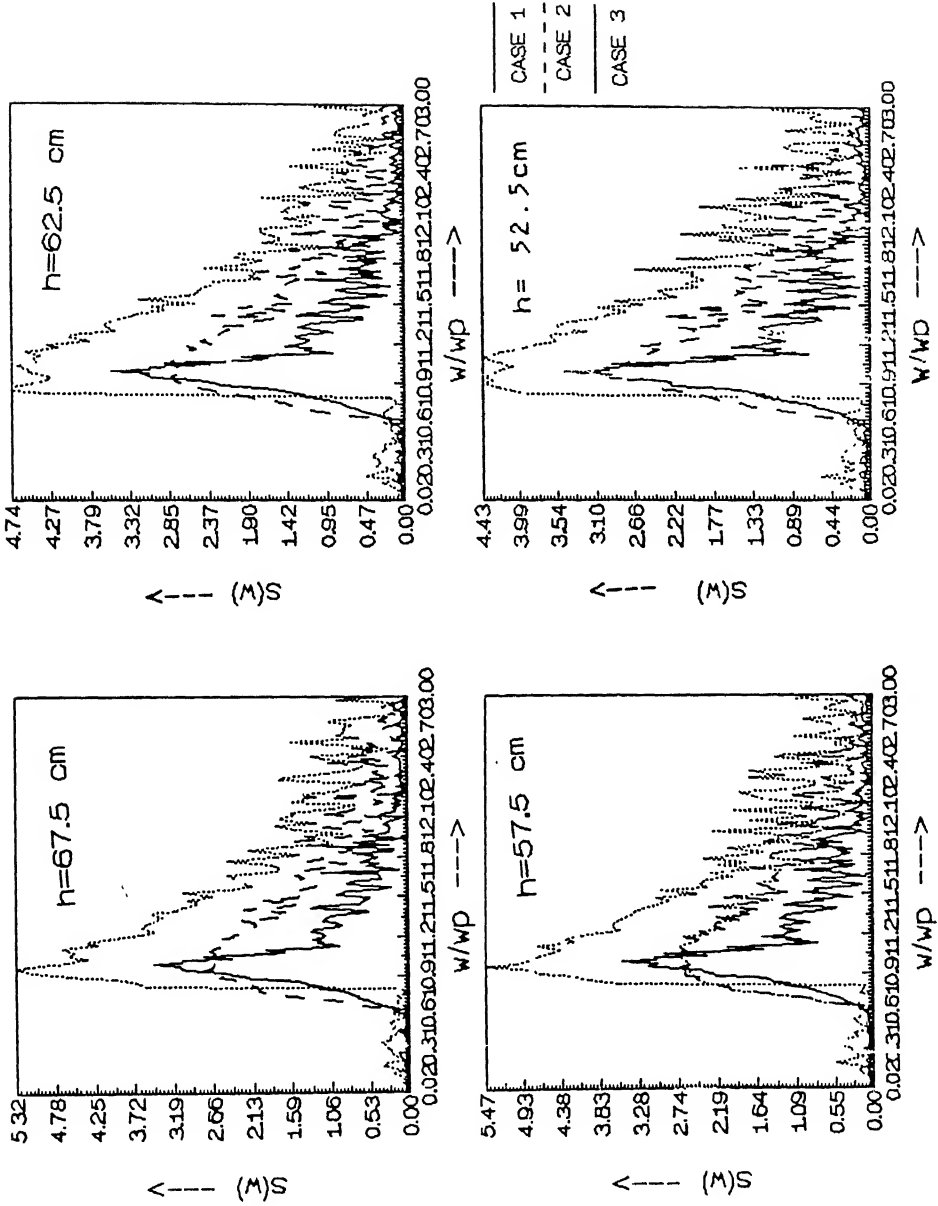


Fig. 4.10 $S(\omega)$ versus ω/ω_p for $h = 67.5$ to 52.5 cm

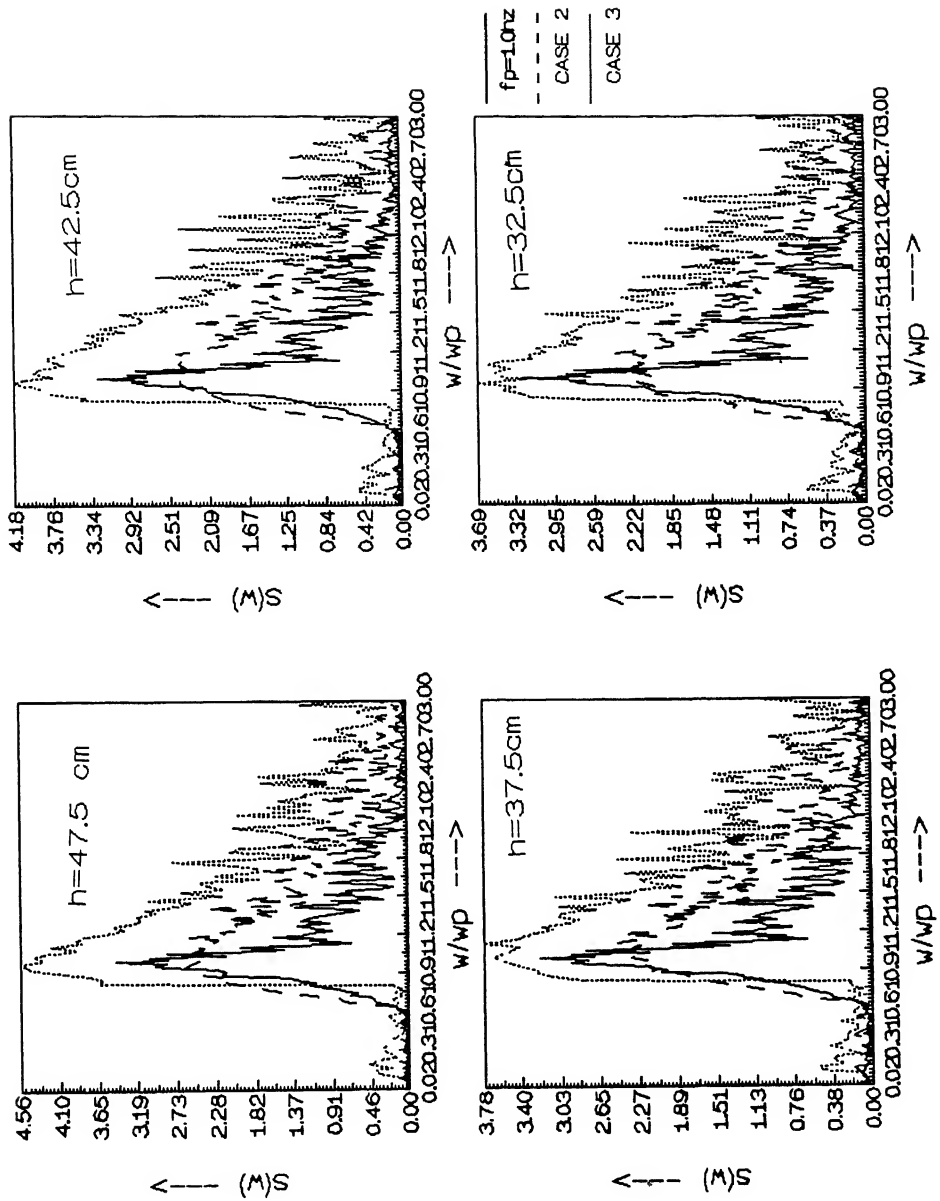


Fig 4.11 $S(\omega)$ versus ω/ω_p for $h = 47.5$ to 32.5 cm

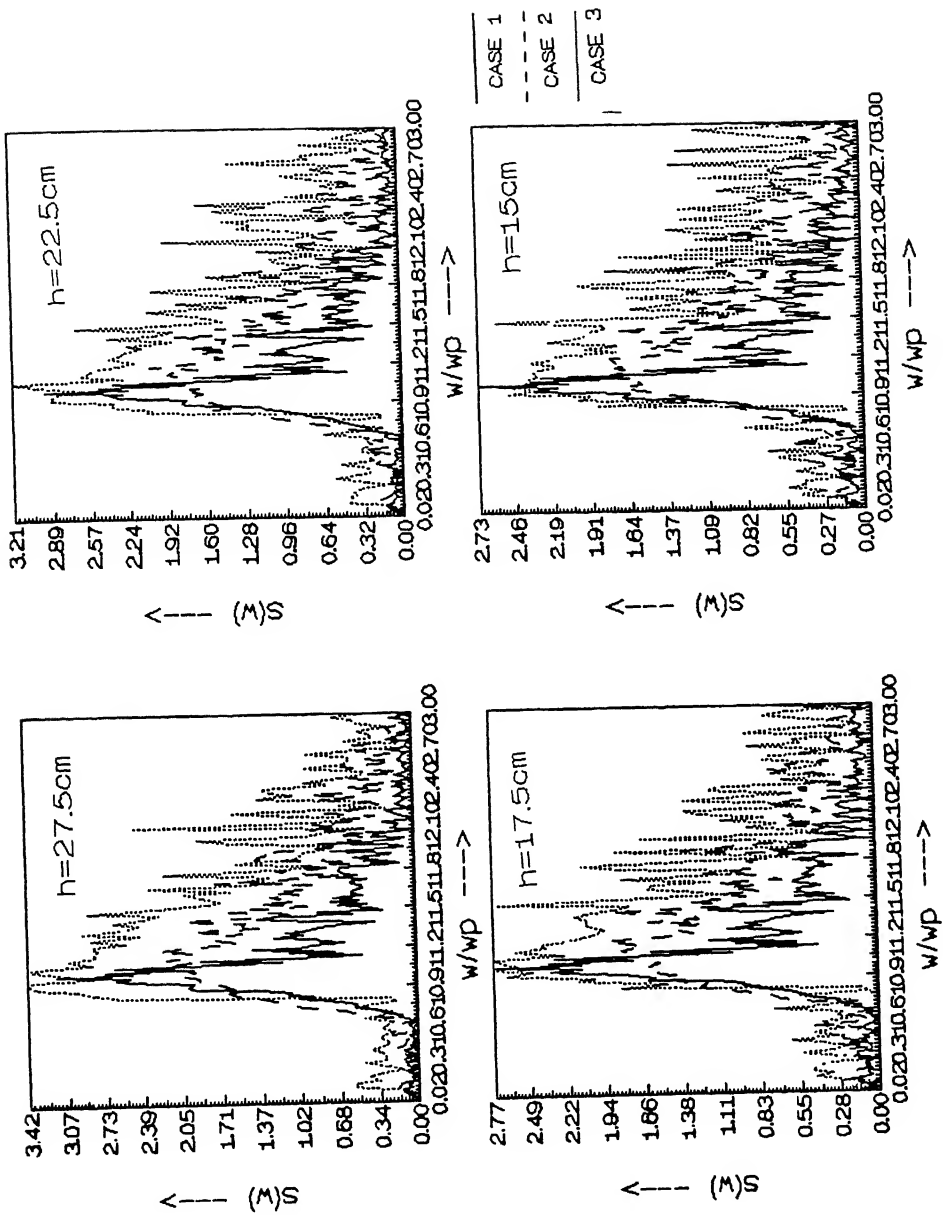


Fig. 4.12 $S(\omega)$ versus w/w_p for $h = 27.5$ to 15.0 cm

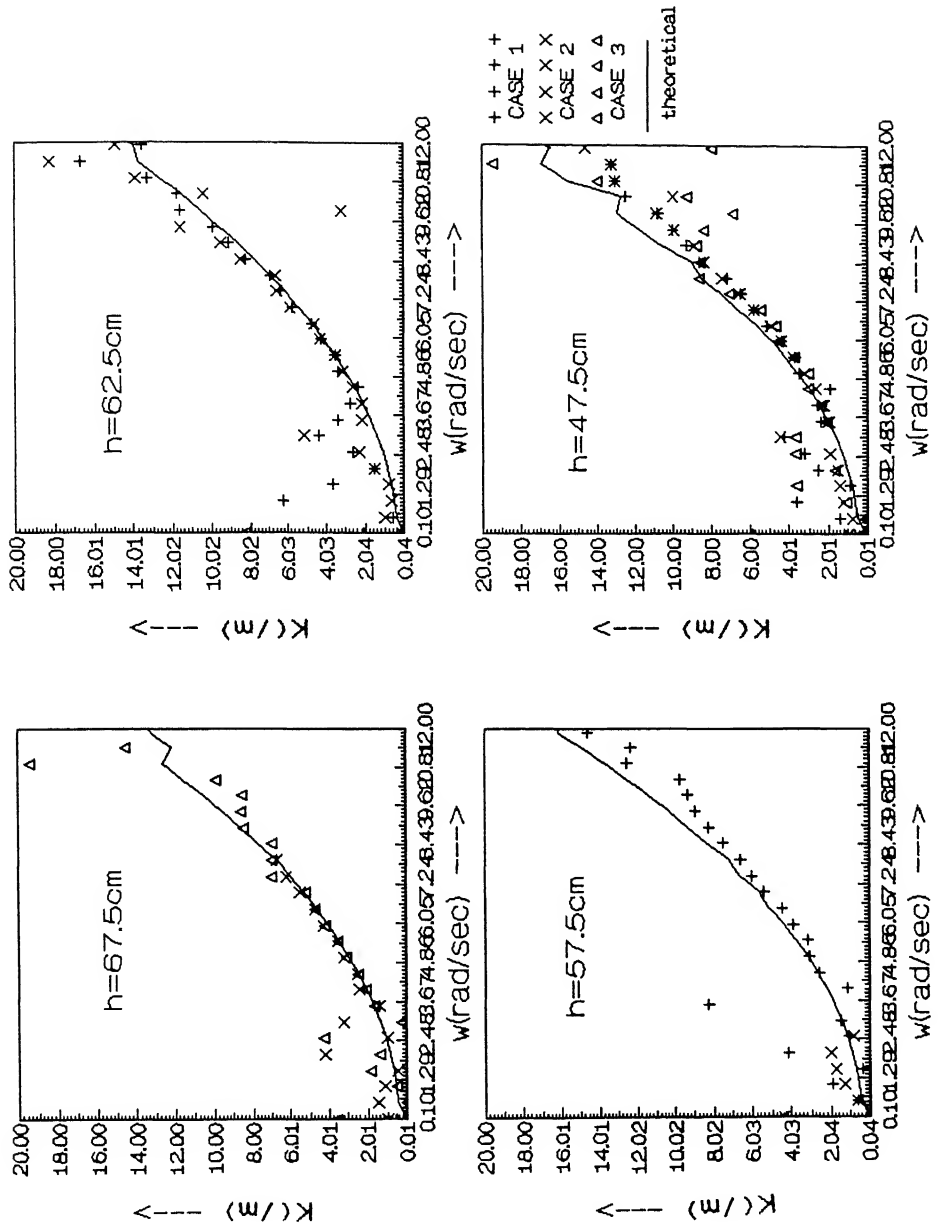


Fig. 4.13 Comparison of theoretical and measured dispersion relation for random waves for $h = 67.5$ to 47.5 cm

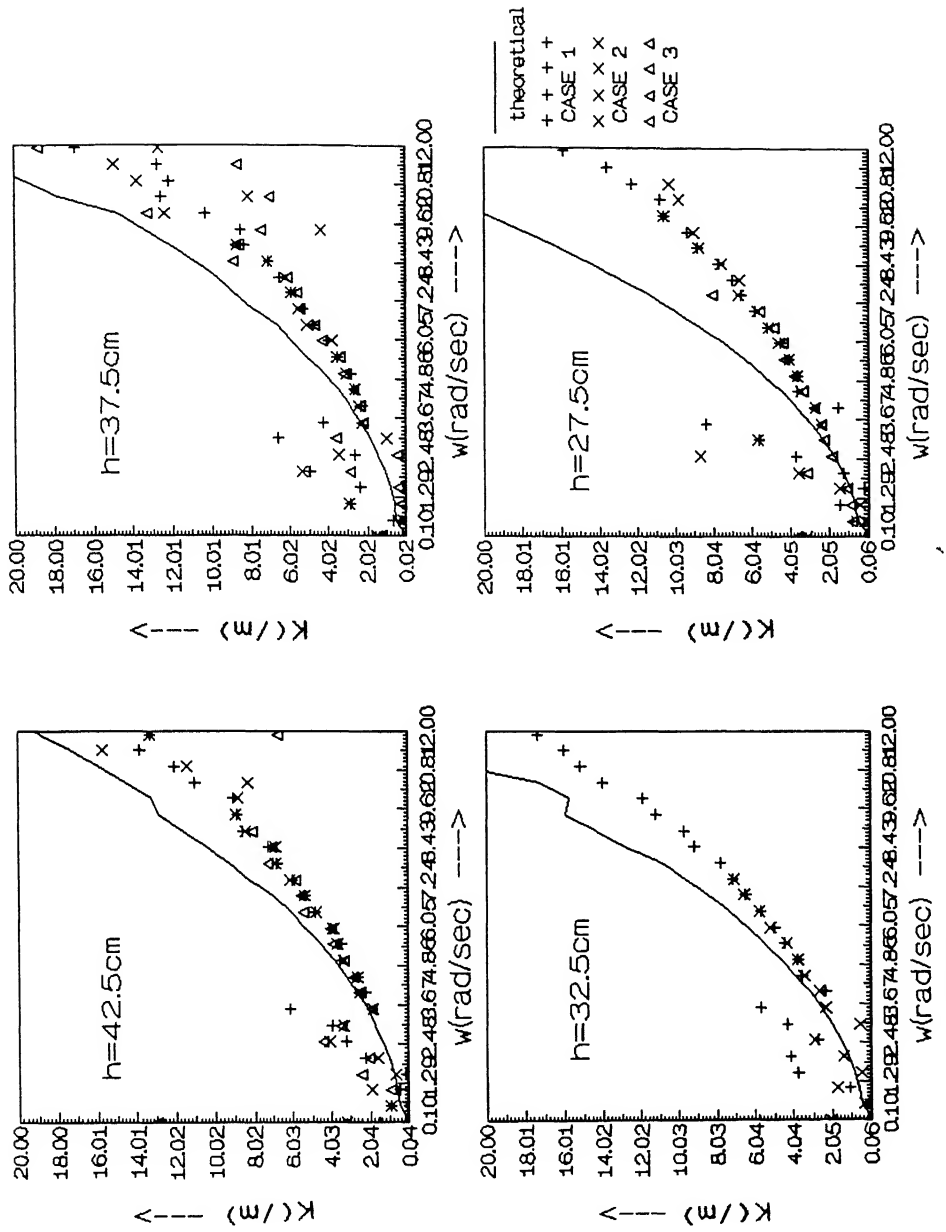


Fig 4.14 Comparison of theoretical and measured dispersion relation for random waves for $h = 42.5$ to 27.5cm

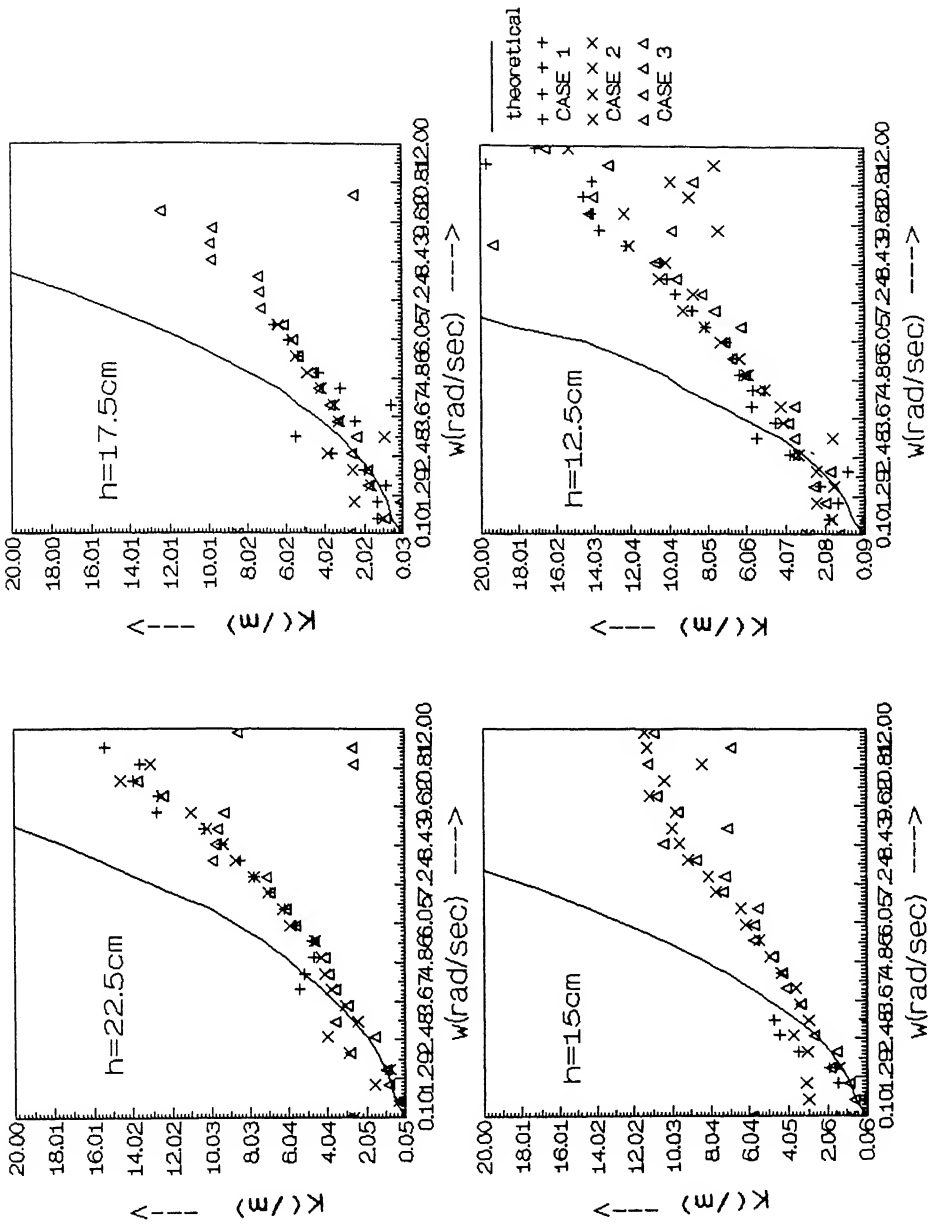


Fig. 4.15 Comparison of theoretical and measured dispersion relation for random waves for $h = 22.5$ to 12.5 cm

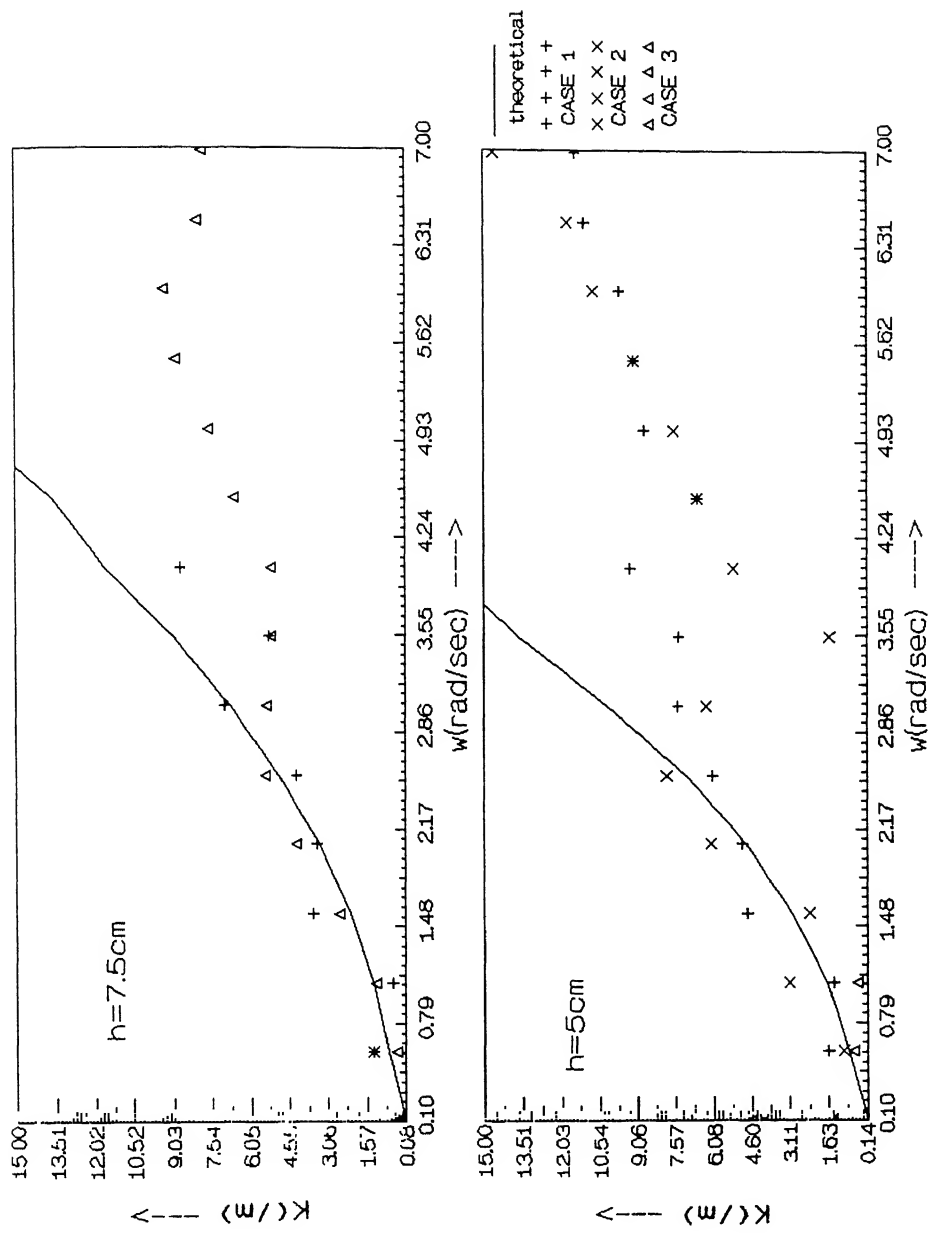


Fig. 4.16 Comparison of theoretical and measured dispersion relation for random waves for $h = 7.5$ to 5.0 cm

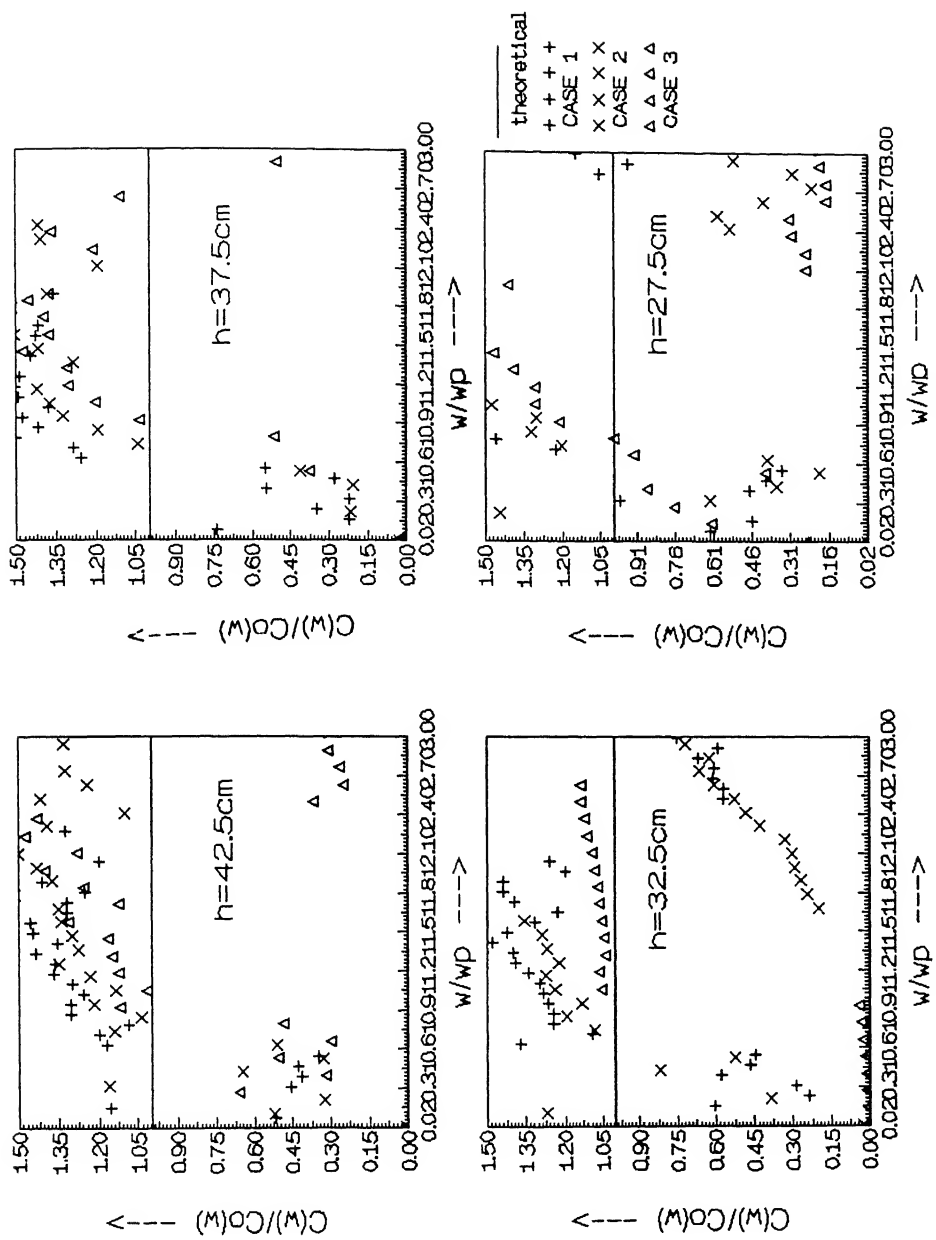


Fig. 4.17 Measured component phase velocity normalised by its deep water value for random waves for $h = 42.5$ to 27.5 cm

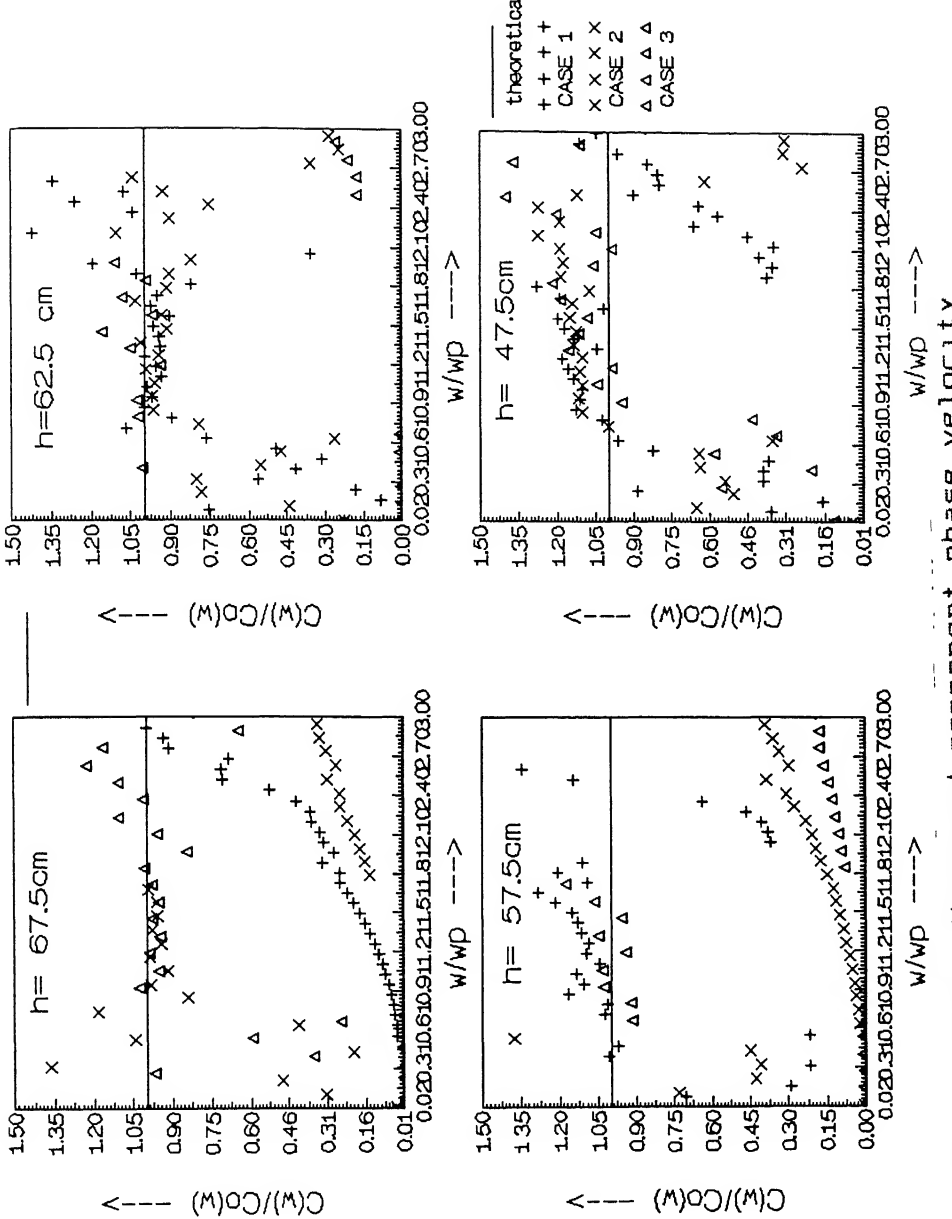


Fig. 4.18 Measured component phase velocity normalised by its deep water value for random waves for $h = 67.5$ to 90 cm

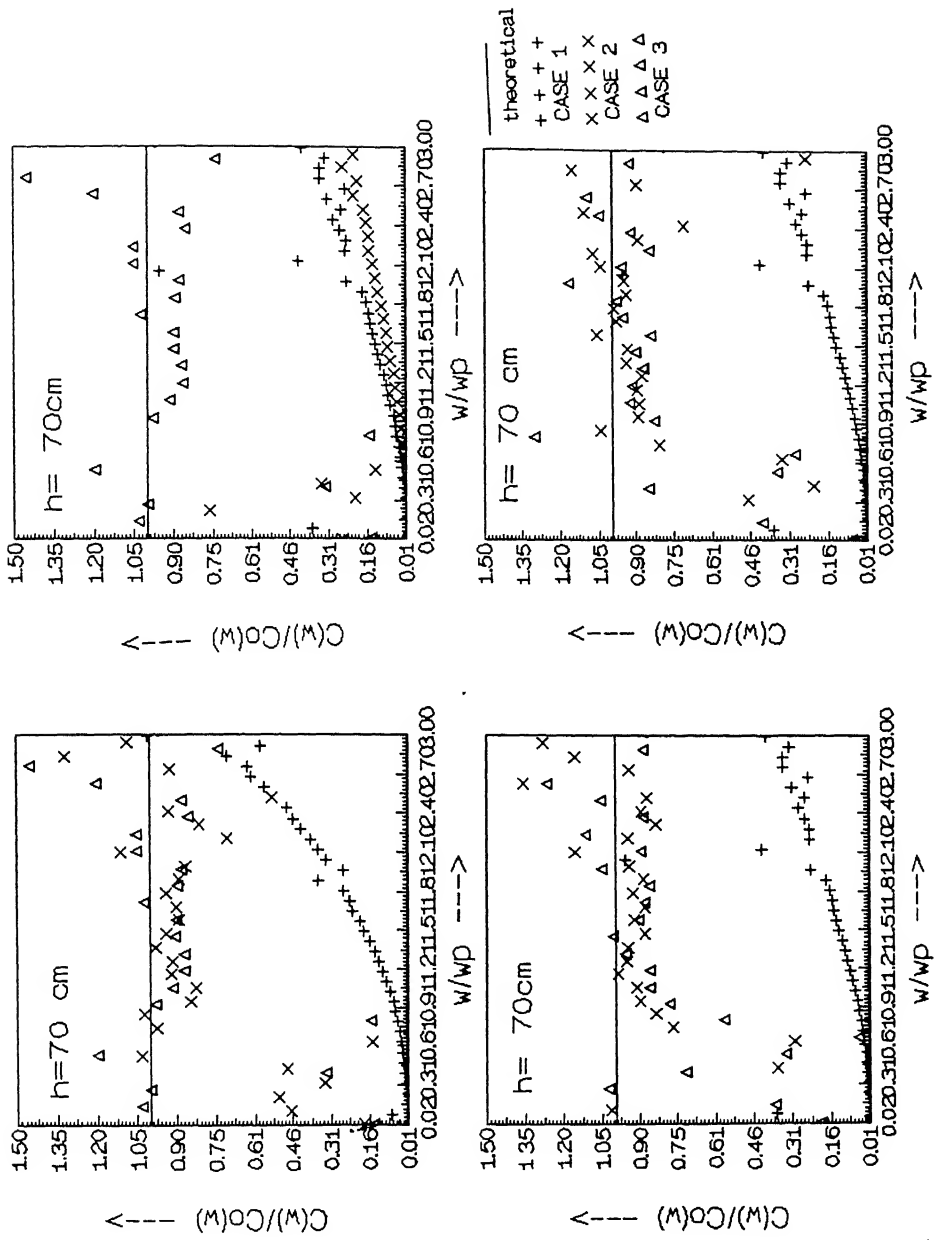


Fig. 4.19 Measured component phase velocity normalised by its deep water value for random waves for $h = 70.0$

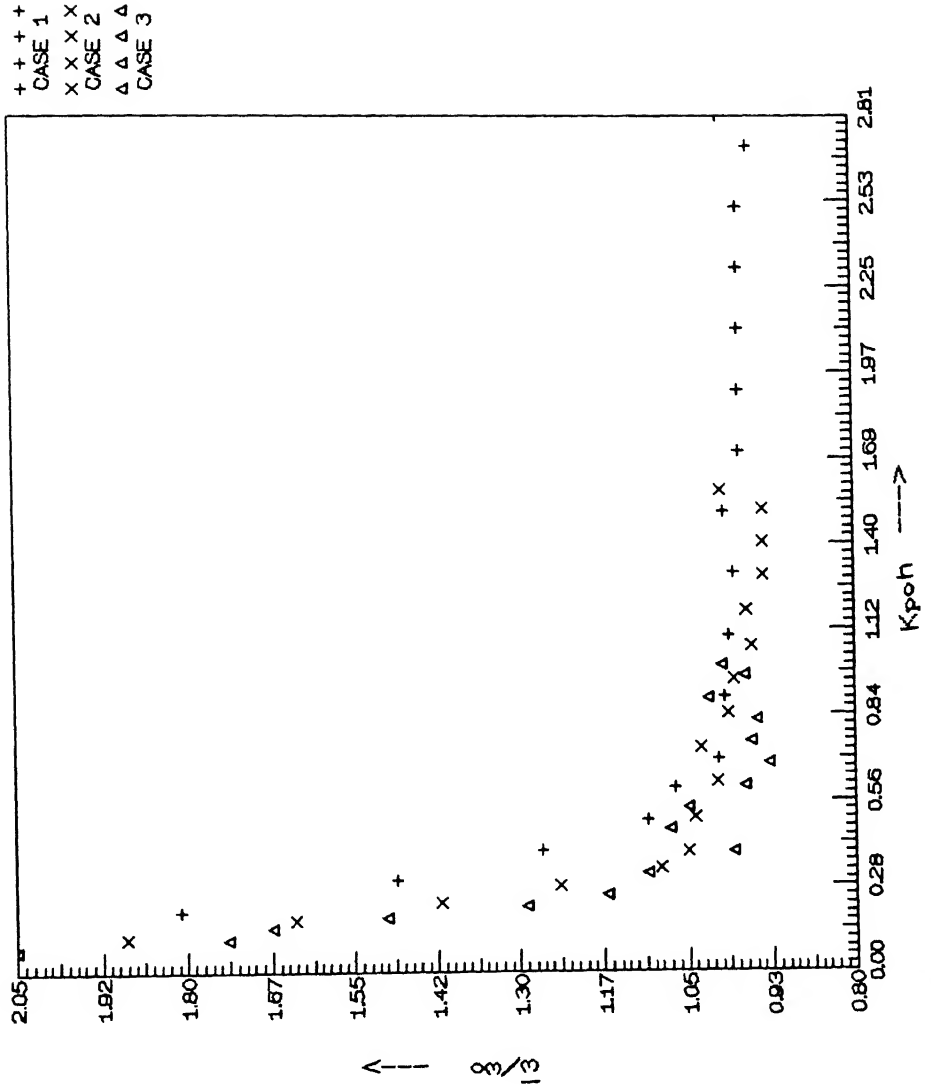


Fig. 4.20 $\bar{\omega}/\omega_0$ versus $K_{\text{波}n}$ (Experimental results)

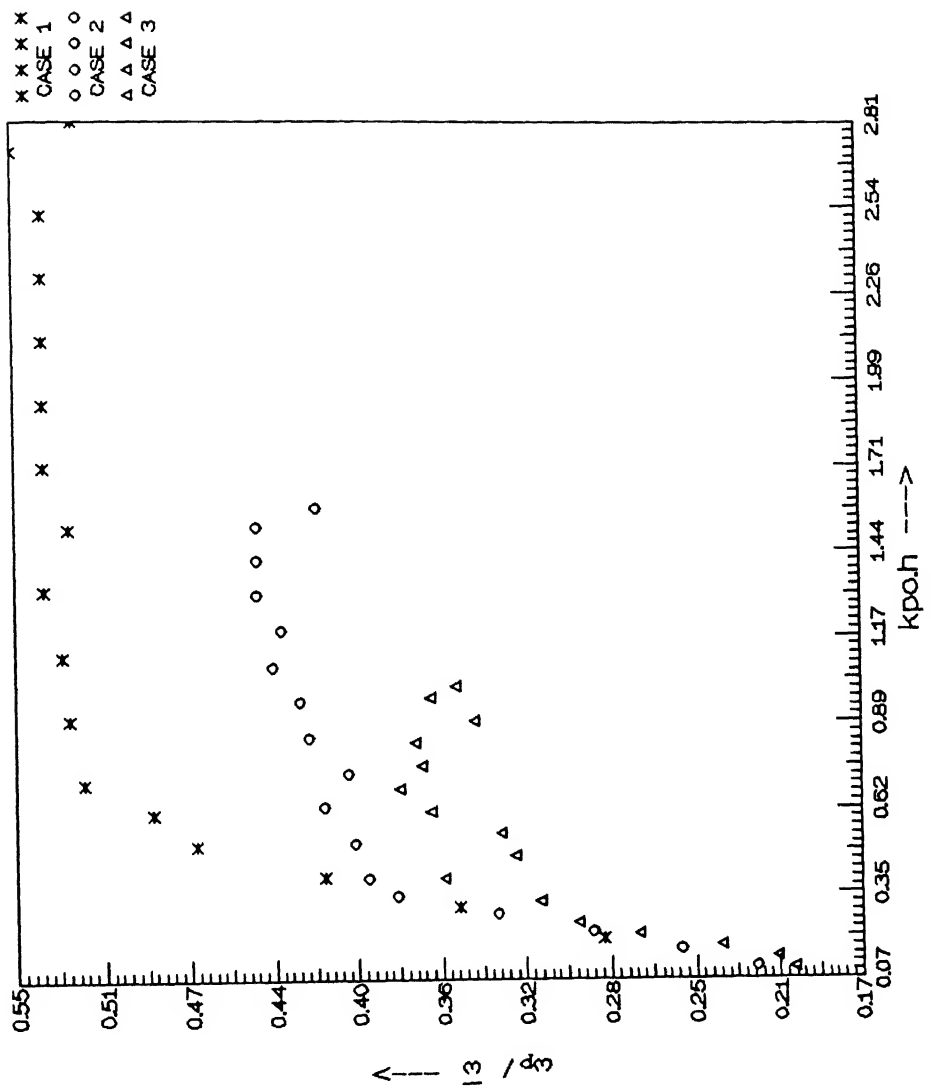


Fig. 4.21 $\omega_p / \bar{\omega}$ versus K_{poh}

Chapter V

CONCLUSIONS

The following conclusions have been drawn in the present study.

- (1) For regular waves the experimental results regarding phase velocity for slope 1:20 are quite close to that of theoretical results by small amplitude wave theory. There is a considerable deviation in terms of wave height.
- (2) (i) For random waves a departure from the theoretical dispersion relation is found in the experiments. This departure increases with decrease in water depth.
(ii) The mean frequency $\bar{\omega}$ increases with decreasing water depth.
(iii) The peak of power spectra of wave height decreases as water depth decreases.

REF E R E N C E S

1. Ayyar, Harihar Raman, Periodic Wave Shoaling in Water in Steeply Sloping Bottom, Proc. of the 12th Int. Conf. on Coast. Eng., 1:22:363-371, 1970.
2. Bendykowska, G. and Werner, Gosta, Transformation of Shallow Water Wave Spectra, Proc. of the 21st Int. Conf. on Coast. Eng., 1:44:612-623, 1988.
3. Ippen, A. T., Estuary and Coastal Hydrodynamics, McGraw Hill, Inc., 1966.
4. Iversen, H.W., Laboratory Study of Breakers, National Bureau of Standards, Circular 521, Washington D.C., 1952, pp. 9-32.
5. Nelson, R. C., The Effect of Bed Slope on Wave Characteristics, Proc. of the 18th Int. Conf. on Coast. Eng., 1:36:555-572, 1982.
6. Sakai, Testuo and Iwagaki, Yuichi, Transformation of Shallow Waves in Shoaling, Proc. of the 14th Int. Conf. on Coast. Eng., 1:23:412-430, 1974.
7. Sarpkaya, Turgut and Isaacson, Michel, Mechanics of Wave Forces on Offshore Structures, Litton Educational Publishing, Inc., 1981.

8. Singamsetti, S. R. & Wind, H. G., Characteristics of Shoaling and Breaking Periodic Waves Normally Incident to Plane Beaches of Constant Slope, Delft Hydraulics Laboratory, July 1980.

9. Svendsen Ib A. and Hansen, T. Buhr, Deformation upto Breaking of Periodic Waves on a Beach, Proc. of the 15th Int. Conf. on Coast. Eng., 1:27:477-497, 1976.

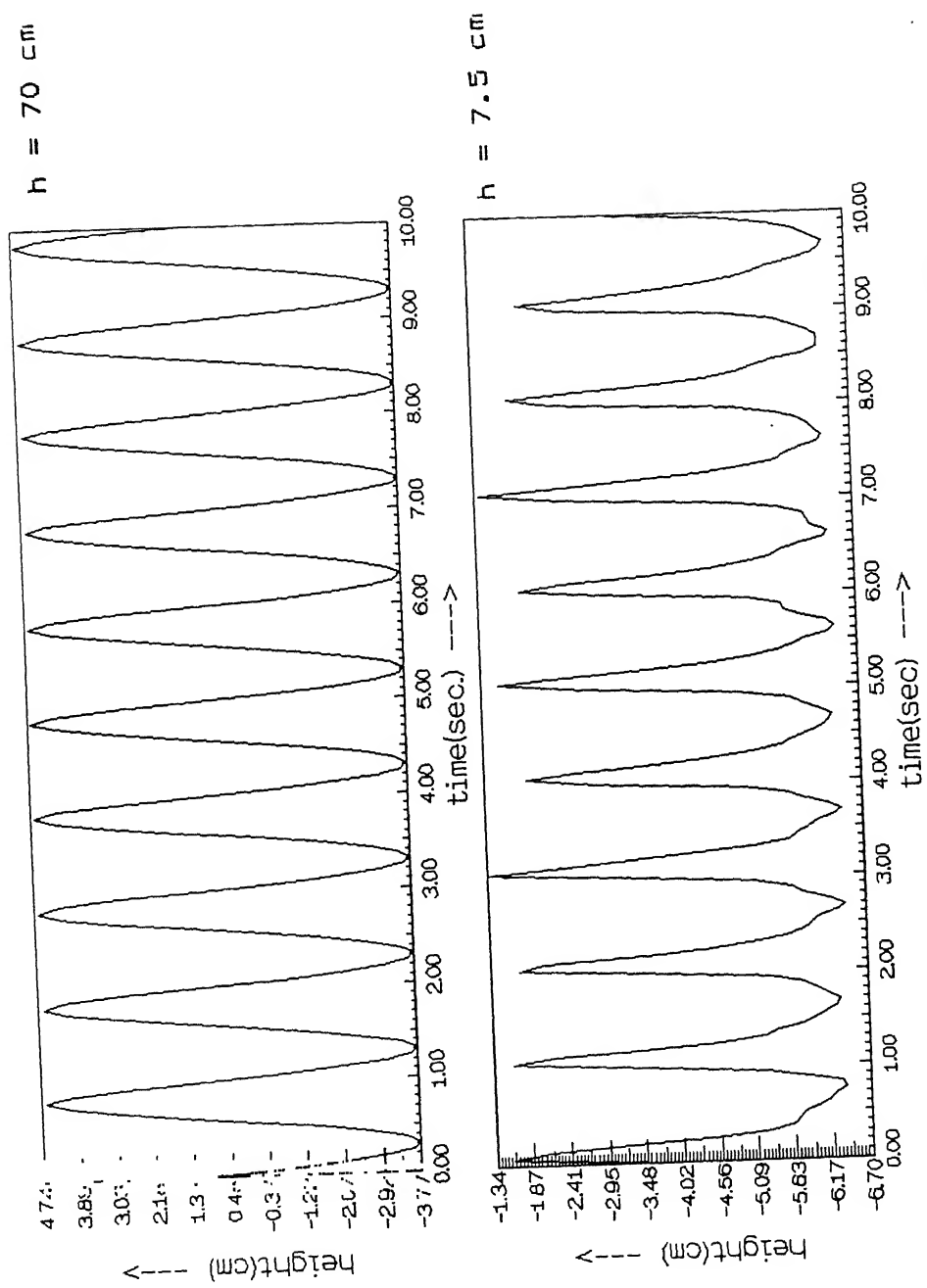


Fig. A.1 Water surface records for regular waves

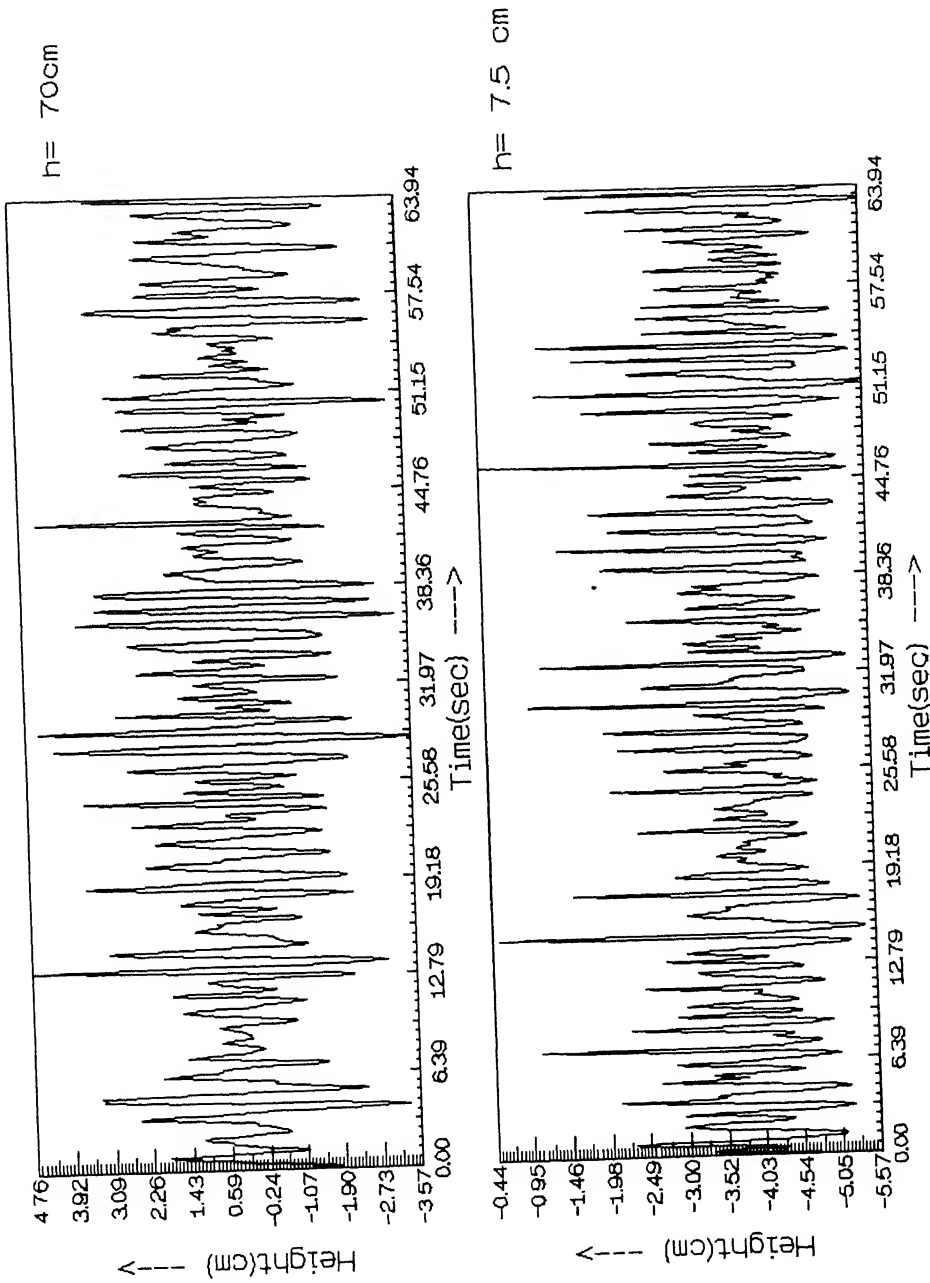


Fig. A.3 Water surface records for random waves (CASE 2)

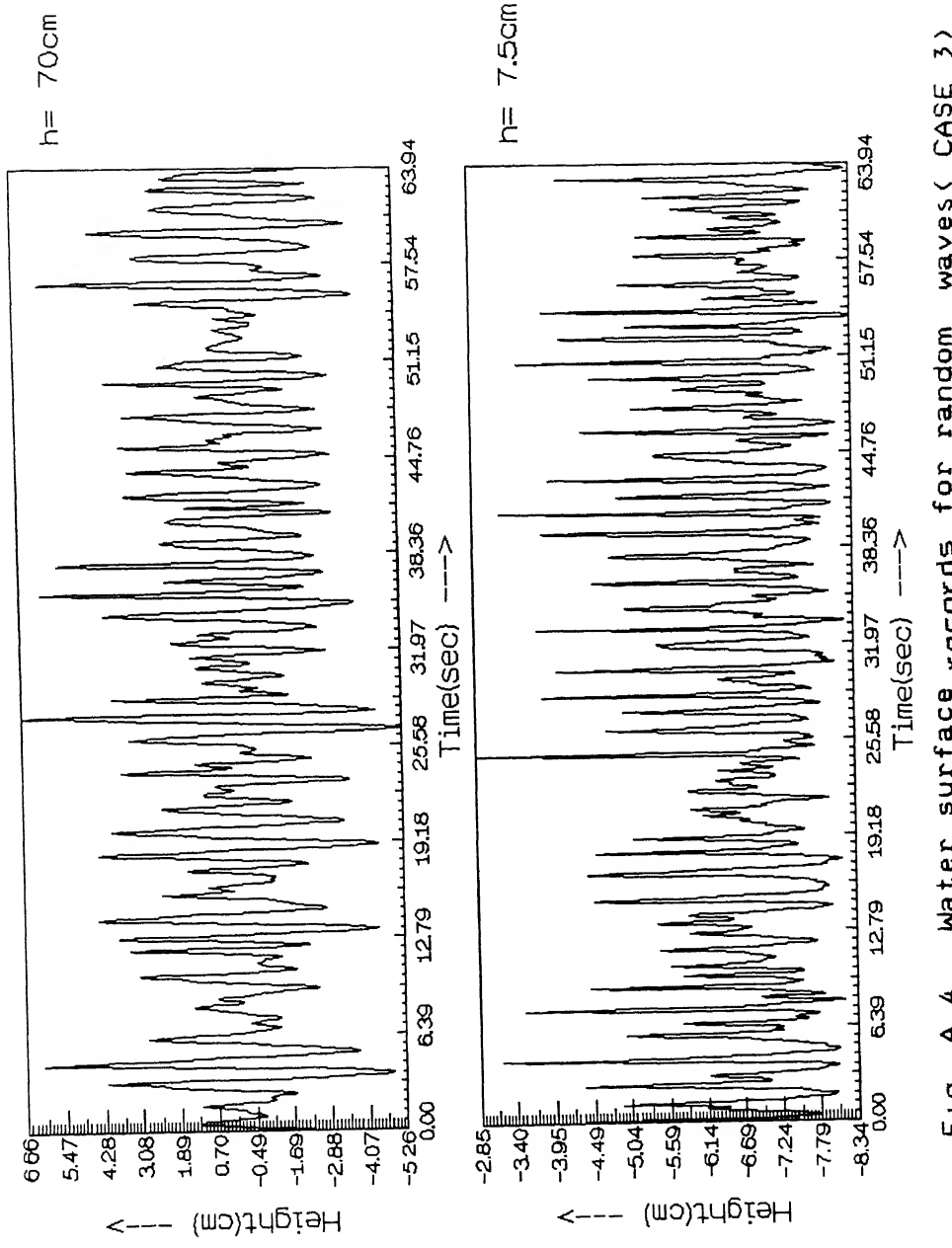


Fig. A.4 Water surface records for random waves (CASE 3)

APPENDIX B

DEFINITIONS OF IMPORTANT PARAMETERS AND METHOD OF THEIR CALCULATION

WAVE CELERITY— is velocity of individual harmonic waves. It is calculated by using the phase difference between the two signals reaching the two probes at any time. It is denoted by C.

WAVE NUMBER is number of waves present per unit length of wave. It is given as,

$$K = \omega / C$$

GROUP VELOCITY is the speed of propagation of a finite group of waves. This is the velocity by which energy is transferred in the direction of wave propagation. When calculated using small amplitude wave theory, one gets,

$$C_g = 0.5 \left[1 + (2Kh) / \sinh(2Kh) \right] C$$

ENERGY FLUX is the average rate of energy transfer per unit width across a plane of constant cross-section.

For regular waves it can be calculated by using small amplitude wave theory from the formula,

$$P = E \cdot Cg$$

Where E = Average energy density

$$= \frac{1}{2} \rho g H^2$$

For random waves

$$P = \rho g \int_0^\infty Cg S(f) df$$

SPECTRAL WIDTH PARAMETER is a measure of non-randomness of a irregular wave and is given by

$$\epsilon = \left(1 - \frac{m_2}{m_0 m_4} \right)^{1/2}$$

Where

$$m_n = \int_0^\infty \omega^n S(f) df$$

PROBABILITY DENSITY FUNCTION - For any stationary signal $x(t)$

$$P(x) = \lim_{T \rightarrow \infty} [T_x / (\Delta x T)]$$

where T_x is the time during which the signal amplitude lies between x and $(x + \Delta x)$ and T is total signal time.

For a random signal $P(x)$ tends towards some limited value as T approaches infinity.

$$P(x) = \lim_{T \rightarrow \infty} \left(\lim_{T_x \rightarrow \infty} (T_x / \Delta x T) \right)$$

Power spectral density function is a measure of energy contained within the signal in each frequency.

If $x(t, f, \Delta f)$ is that part of signal $x(t)$ which lies in frequency band Δf centred at frequency f , then the mean square value within this band is

$$S^2(f) = \lim_{T \rightarrow \infty} \left[\frac{1}{T} \int_0^T x^2(t, f, \Delta f) dt \right]$$

The power spectral density can be defined by

$$E(f) = \lim_{T \rightarrow \infty} [S^2(f) / \Delta f \bar{x}^2]$$

Where \bar{x}^2 is the total mean square. In practice, $E(f)$ is found using Fourier transform.

APPENDIX C

LISTING OF PROGRAMMES

CONVERSION OF VOLTAGE SIGNALS TO ELEVATION SIGNALS

```

dimension a1(1100),a2(1100),b1(1100),b2(1100),time(1100)
common / calib / v(40,2),h(40,2),n1,n2
print *, 'specify number of calibration points for probes 1 & 2'
read *, n1,n2
open(unit=12,file='calib.dat',status='old')
read(12,*) (v(i,1),h(i,1),i=1,n1)
read(12,*) (v(i,2),h(i,2),i=1,n2)
close(unit=12,status='keep')

nu=10
n=2**nu
pi=3.1415926

open(unit=8,file='p.dat',status='old')
read(8,*) (time(i),a1(i),i=1,n)
read(8,*) (time(i),a2(i),i=1,n)
close(unit=8,status='keep')

do 10 i=1,n
a1(i)=10.0*a1(i)
a2(i)=10.0*a2(i)
b1(i)=convert(a1(i),1)
b2(i)=convert(a2(i),2)
continue

open(unit=16,file='ph.dat',status='unknown')
write(16,111) (time(i),b1(i),i=1,n)
format(1x,f12.5,8x,f12.5)
write(16,211) (time(i),b2(i),i=1,n)
format(1x,f12.5,8x,f12.5)
close(unit=16,status='keep')

stop
end

function convert(x,ip)
common / calib / v(40,2),h(40,2),n1,n2

if(ip.eq.1) n=n1
if(ip.eq.2) n=n2
do 10 i=1,n-1
if(x.lt.v(i,ip).and.x.ge.v(i+1,ip)) go to 100
continue
print *, 'interpolation failure'
print *, 'probe number',ip
print *, x
stop
grad=(h(i+1,ip)-h(i,ip))/(v(i+1,ip)-v(i,ip))
convert=h(i,ip)+grad*(x-v(i,ip))

return
end

```

APPENDIX C

LISTING OF PROGRAMMES

C CONVERSION OF VOLTAGE SIGNALS TO ELEVATION SIGNALS

```

dimension al(1100),a2(1100),b1(1100),b2(1100),time(1100)
common / calib / v(40,2),h(40,2),n1,n2

print *, 'specify number of calibration points for probes 1 &
read *, n1,n2

open(unit=12,file='calib.dat',status='old')
read(12,*) (v(i,1),h(i,1),i=1,n1)
read(12,*) (v(i,2),h(i,2),i=1,n2)
close(unit=12,status='keep')

nu=10
n=2**nu
pi=3.1415926

open(unit=8,file='p.dat',status='old')
read(8,*) (time(i),al(i),i=1,n)
read(8,*) (time(i),a2(i),i=1,n)
close(unit=8,status='keep')

do 10 i=1,n
al(i)=10.0*al(i)
a2(i)=10.0*a2(i)
b1(i)=convert(al(i),1)
b2(i)=convert(a2(i),2)
10 continue

open(unit=16,file='ph.dat',status='unknown')
write(16,111) (time(i),b1(i),i=1,n)
format(1x,f12.5,8x,f12.5)
write(16,211) (time(i),b2(i),i=1,n)
format(1x,f12.5,8x,f12.5)
close(unit=16,status='keep')

stop
end

function convert(x,ip)
common / calib / v(40,2),h(40,2),n1,n2

if(ip.eq.1) n=n1
if(ip.eq.2) n=n2
do 10 i=1,n-1
if(x.lt.v(i,ip).and.x.ge.v(i+1,ip)) go to 100
10 continue
print *, 'interpolation failure'
print *, 'probe number',ip
print *, x
stop
100 grad=(h(i+1,ip)-h(i,ip))/(v(i+1,ip)-v(i,ip))
convert=h(i,ip)+grad*(x-v(i,ip))

return
end

```

```

C PROGRAMME TO CALCULATE WAVENUMBER & CELERITY FOR RANDOM WAVE
C CALCULATION OF POWER SPECTRUM OF SIGNALS USING FFT.
C CALCULATION OF PHASE DIFFERENCE BETWEEN TWO SIGNALS.

dimension a1(1100),a2(1100),b(1100),power1(1100),power2(1100)
dimension a11(1100),a22(1100)
complex x1(1100),x2(1100)
dimension pl2(1100),time(1100),pcr(1100),pl1(1100),p22(1100)
dimension ak(1100),cel(1100),phased(1100)
dimension w(1100)

pi=3.1415
nu=10
delx=.10

n=2**nu
pi=3.1415926

open(unit=8,file='ph.dat',status='old')
read(8,*) (time(i),a11(i),i=1,n)
read(8,*) (time(i),a22(i),i=1,n)
scale=1.0
do 20 i=1,n
a1(i)=a11(i)*scale
a2(i)=a22(i)*scale
continue
close(unit=8,status='keep')

20 del=time(2)-time(1)
tt=del*(n-1)

call fft(a1,b,x1,nu,del)
call fft(a2,b,x2,nu,del)

C CALCULATION OF COHERENCE FUNCTION AND PHASE ANGLE.

do 100 i=1,n/2
rl=real(x1(i))
s1=imag(x1(i))
r2=real(x2(i))
s2=imag(x2(i))
pl1(i)=atan(s1/r1)

p22(i)=atan(s2/r2)
if (rl.lt.0.and.s1.gt.0) pl1(i)=pl1(i)+ pi
if (rl.lt.0.and.s1.lt.0) pl1(i)=pl1(i)+ -pi
if (rl.gt.0.and.s1.lt.0) pl1(i)=pl1(i)+ 2*pi
if (r2.lt.0.and.s2.gt.0) p22(i)=p22(i)+ pi
if (r2.lt.0.and.s2.lt.0) p22(i)=p22(i)+ -pi
if (r2.gt.0.and.s2.lt.0) p22(i)=p22(i)+ 2*pi

t1=r1*r2+s1*s2
t2=s1*r2-r1*s2

pcrm=sqrt(t1**2+t2**2)
power1(i)=sqrt(r1**2+s1**2)
power2(i)=sqrt(r2**2+s2**2)
pcr(i)=pcrm/(power1(i)*power2(i))
100 continue

do 50 i=7,n/2,5
if (pl1(i).gt.pl1(i-5)) go to 50
pl1(i)=pl1(i)+2*pi
go to 25
50 continue

do 60 i=7,n/2,5
if (p22(i).gt.p22(i-5)) go to 60
p22(i)=p22(i)+2*pi
60 continue

```

```

do 63 i=2,n/2,5
p12(i)=abs(p11(i)-p22(i))
continue

open(unit=17,file='ax')
write(17,555)(p11(i),p22(i),p12(i),i=2,n/2,5)
format(3x,f12.5,8x,f12.5,4x,f12.5)
pmax=1.0e-08
do 56 i=2,n/2,5
pmax1amax1(powerl(i),pmax)
if(pmax.ne.pmax1) ii=i
pmax=pmax1
continue
print *, 'maximum power and location', powerl(ii),ii
do 51 i=2,n/2,5
phased(i)=p12(i)
ak(i)=phased(i)/delx
cel(i)=2.0*p1*b(i)/ak(i)
continue

do 39 i=2,n/2,5
w(i)=2*p1*b(i)
continue

open(unit=7,file='output')
write(7,222)(w(i),ak(i),i=2,430,5)
format(3x,f12.5,8x,f12.5)

open(unit=13,file='input')
write(13,333)(w(i),cel(i),i=2,430,5)
format(3x,f12.5,8x,f12.5)
print*, 'coherence factor',pcr(ii)

delf=1.0/tt

open(unit=22,file='power.dat',status='unknown')
fnyquist=1.0/(2.0*del)
do 85 i=1,n
if(b(i).ge.fnyquist) go to 86
continue
ij=i
write (22,1130)
format(/2x,'frequency in Hz; amplitude cmsquare.sec',//)
write(22,1100)
format(5x,'frequency',11x,'amplitude',12x,'phase',//)
write(22,1150) (b(i),powerl(i),power2(i),p12(i),i=1,ij)
format(3x,e12.5,4x,e12.5,4x,e12.5,4x,e12.5)
write(22,1190) fnyquist
format(/5x,'Nyquist frequency=',e12.5)
close(unit=22,status='keep')

stop
end

```

```

subroutine fft(a,b,x,nu,del)
dimension x(1100),b(1100),a(1100)
complex x,u,w,t
n=2**nu
pi=3.141592653
tt=(n-1)*del

do 5 jj=1,n
b(jj) = (jj-1)/tt
continue
5

do 6 i=1,n
x(i)=cmplx(a(i),0.0)
continue
6

do 20 l=1,nu
le=2**((nu+l-1)
lcl=le/2
u=(1.,0.)
w=cmplx(cos(pi/float(lcl)),-sin(pi/float(lcl)))
do 20 j=1,lcl
do 10 i=j,n,le
ip=i+lcl
t=x(i)+x(ip)
x(ip)=(x(i)-x(ip))*u
x(i)=t
u=u*w
10
20

nv2=n/2
nm1=n-1
j=1
do 30 i=1,nm1
if(i.ge.j)go to 25
t=x(j)
x(j)=x(i)
x(i)=t
25
35
if(k.ge.j)go to 30
j=j-k
k=k/2
go to 35
30
j=j+k

return
end

subroutine trap(x,n,e)
dimension x(1100)

fx=0.0
do 10 i=2,n-1
fx=fx+x(i)
continue
10

e=(x(1)+x(n)+2.0*fx)/(2.0*(n-1))

return
end

```

```

c      PROGRAMME TO CALCULATE WAVE SPECTRUM

dimension a(3200),power(3200),auto(3200),alag(3200)
dimension b(3200),a2(3200),time(3200)
complex x(3200)
common / tr /troom

print *, 'what are nu ndata del'
read *, nu,ndata,del
scale=1.0

n=2**nu
tt=del*(n-1)
pi=3.1415926

open(unit=21,file='p',status='old')
read(21,*) (time(i),a(i),i=1,ndata)
close(unit=21,status='keep')

c      remove  stray mean.

call trap(a,ndata,e)
do 65 i=1,ndata
a(i)=a(i)-e
continue

c      filter data (Tukey- Hanning formula).

ttl=0.5*del*(ndata-1)
do 75 i=1,ndata
tl=del*(i-1)
wt=1.0
a2(i)=a(i)**2
a(i)=a(i)*wt*scale
continue

call trap(a2,ndata,variance)

do 45 i=ndata+1,n
a(i)=0.0
continue .

call fft(a,b,x,nu,del)

do 100 i=1,n
r=real(x(i))
s=imag(x(i))
power(i)=((sqrt(r**2+s**2))/tt)
continue
print *, 'power spectrum calculated'

delf=1.0/tt

open(unit=22,file='pp.dat',status='unknown')
fnyquist=1.0/(2.0*del)
do 85 i=1,ndata
if(b(i).ge.fnyquist) go to 86
continue
i=j
write (22,1130)
format(/2x,'frequency in Hz; amplitude cmsq/sec',//)
write(22,1100)
format(5x,'frequency',11x,'amplitude',//)
write(22,1150) (b(i),power(i),i=1,1)
format(3x,e12.5,8x,e12.5)
write(22,1190) fnyquist
format(/5x,'Nyquist frequency=',e12.5)
close(unit=22,status='keep')

stop
end

```

```
subroutine fft(a,b,x,nu,del)
dimension x(3200),b(3200),a(3200)
complex x,u,w,t
n=2**nu
pi=3.141592653
tt=(n-1)*del

5   do 5 jj=1,n
      b(jj) = (jj-1)/tt
      continue

6   do 6 i=1,n
      x(i)=cmplx(a(i),0.0)
      continue

10  do 20 l=1,nu
      le=2***(nu+l-1)
      le1=le/2
      u=(1.,0.)
      w=cmplx(cos(pi/float(le)),-sin(pi/float(le)))
      do 20 j=1,le1

15  do 10 ip=j,n,le
      ip=j+le1
      t=x(ip)+x(ip)
      x(ip)=(x(ip)-x(ip))*u
      x(ip)=t
      u=u*w

20  nv2=n/2
      nm1=n-1
      j=1
      do 30 i=1,nm1
      if(i.ge.j)go to 25
      t=x(i)
      x(j)=x(i)
      x(i)=t
      k=nv2
      if(k.ge.j)go to 30
      j=j-k
      k=k/2
      go to 35
      j=j+k

25  return
      end

30  subroutine trap(x,n,e)
      dimension x(3200)

10  fx=0.0
      do 10 i=2,n-1
      fx=fx+x(i)
      continue

      e=(x(1)+x(n)+2.0*fx)/(2.0*(n-1))

      return
      end
```

```

c      PROGRAMME TO CALCULATE ENERGY FLUX
dimension cel(1000),ak(1000),cg(1000),w(1000),s(10000)
g=9.81
df=.0156
rho=1000
n=86

print*, "d=?"
read*, d

open (unit=33,file='put')
read(33,*)(cel(i),ak(i),i=1,n)

do i=1,n
cg(i)=0.5*cel(i)*(1+2*ak(i)*d/sinh(2*ak(i)*d))
enddo

open (unit=44,file='output1')
write(44,400) (cel(i),cg(i),i=1,n)
format(1x,f12.5,8x,f12.5)
400

open(unit=55,file='pp.dat')
read(55,*)(w(i),s(i),i=1,n)
sum=0.0

do i=1,86
sum=sum+s(i)*cg(i)
enddo
print*, "sum=",sum

eflux=rho*df*g*sum
print*, "eflux=",eflux

stop
end

```

```
c PROGRAMME TO CALCULATE SPECTRUM WIDTH PARAMETER
dimension f(1000),s(1000)
print*, "df=", df
read*, df
pi=3.1415
dw=2*pi*df

open (unit=7,file='input')
read(7,*)(f(i),s(i),i=1,512)

sum1=0.0
sum2=0.0
sum3=0.0

do i=1,512
sum1= sum1+s(i)
sum2= sum2+(s(i)*(f(i)**2))
sum3= sum3+(s(i)*(f(i)**4))
enddo

print*, "sum1=",sum1
print*, "sum2=",sum2
print*, "sum3=",sum3

sigmasquare=(1-(sum2/(sum1*sum3*df)))
print*, "sigmasquare",sigmasquare

stop
end
```

c PROGRAMME TO GENERATE REGULAR WAVE

```
#include <default.h>
#include <default.ttf>
#include <macros.h>
```

```
run "1 hz wave 0.05m" with
    OneFreq_0(1.0,0.05)
    sample "Waveguage 31 Jan 1994" on 0
end
```

c regular wave parameters frequency=1 Hz
amplitude=5 cm

c PROGRAMME TO GENERATE RANDOM WAVE

```
#include <default.h>
#include <default.ttf>
#include <macros.h>

wave w1 = jonswap(0.75,0.0081,1.0,0.07,0.09)
wave w2 = random(w1,1)

run "Jonswap spectrum" with
    wavemaker w2 with TTF on 0
    sample "Waveguage (P1) 01 Mar 1994" on 0
    sample "Wavegauge (P2) 01 Mar 1994" on 0
end
```

c jonswap parameters peak frequncy = .75 Hz
 alpha = .0081
 gamma = 1.0
 sigma a = .07
 sigma b = .09